



NON-CLASSICAL CARBONYL COMPLEXES OF
ZIRCONIUM: THE SYNTHESSES, CHARACTERIZATION,
AND REACTIVITIES OF $(\eta^5\text{-C}_5\text{Me}_5)_2\text{Zr}(\eta^2\text{-E}_2)(\text{CO})$
(E = S, Se, Te)*

WILLIAM A. HOWARD and GERARD PARKIN†

Department of Chemistry, Columbia University, New York, NY 10027, U.S.A.

and

ARNOLD L. RHEINGOLD

Department of Chemistry, University of Delaware, Newark, DE 19716, U.S.A.

Abstract—The non-classical zirconium carbonyl complexes $\text{Cp}_2^*\text{Zr}(\eta^2\text{-E}_2)(\text{CO})$ (E = S, Se, Te) have been prepared by the reactions of $\text{Cp}_2^*\text{Zr}(\text{CO})_2$ with the elemental chalcogens (*ca.* two equivalents) at *ca.* 80°C. $\text{Cp}_2^*\text{Zr}(\eta^2\text{-E}_2)(\text{CO})$ are characterized by ν_{CO} stretching frequencies of 2057 cm^{-1} (E = S), 2037 cm^{-1} (E = Se) and 2006 cm^{-1} (E = Te), and the ditellurido derivative $\text{Cp}_2^*\text{Zr}(\eta^2\text{-Te}_2)(\text{CO})$ has been structurally characterized by X-ray diffraction. The dichalcogenido-carbonyl complexes $\text{Cp}_2^*\text{Zr}(\eta^2\text{-E}_2)(\text{CO})$ (E = S, Se, Te) react further with excess chalcogen to give the trichalcogenido complexes $\text{Cp}_2^*\text{Zr}(\eta^2\text{-E}_3)$, which have also been structurally characterized by X-ray diffraction. The formation of the tritellurido complex $\text{Cp}_2^*\text{Zr}(\eta^2\text{-Te}_3)$ is reversible, and addition of CO (1 atm) regenerates $\text{Cp}_2^*\text{Zr}(\eta^2\text{-Te}_2)(\text{CO})$. In the presence of pyridine, the dichalcogenido derivatives $\text{Cp}_2^*\text{Zr}(\eta^2\text{-E}_2)(\text{CO})$ react with $\text{Cp}_2^*\text{Zr}(\text{CO})_2$ to give the terminal chalcogenido complexes $\text{Cp}_2^*\text{Zr}(\text{E})(\text{NC}_5\text{H}_5)$. $\text{Cp}_2^*\text{Zr}(\eta^2\text{-Te}_2)(\text{CO})$ exists in both triclinic and tetragonal modifications. Interestingly, the derived Zr—CO bond lengths for the two structures were significantly different, while the C—O bond lengths for each structure were similar. The origin of the discrepancy was determined to be crystallographic disorder in the tetragonal modification, and appropriate modeling allowed the derivation of a reasonable Zr—CO bond length for the tetragonal form.

Metal carbonyl complexes are ubiquitous in organo-transition metal chemistry and the nature of the [M—CO] interaction has been the subject of many investigations.^{1,2} On the basis of these studies, it is commonly accepted that the bonding of CO to a transition metal center comprises the synergistic interaction of ligand-to-metal σ -donation and

metal-to-ligand π -back-bonding.³ Indeed, since CO is only a weak σ -donor ligand, the metal-to-ligand $d \rightarrow \pi^*$ interaction provides an important contribution to the strength of the M—CO bond.⁴ As a consequence, transition metal carbonyl complexes typically possess metal centers in which there is a supply of d electrons (i.e. $d^{>0}$) available for back-bonding. Nevertheless, $d \rightarrow \pi^*$ back-bonding should not be regarded as a prerequisite for CO binding, since a number of carbonyl complexes of the main group elements are known for which back-bonding is either non-existent or very weak. Some examples of such carbonyl adducts include

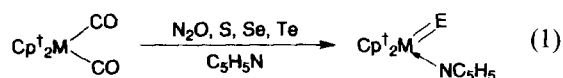
* Dedicated to Professor John E. Bercaw (EQG), an outstanding chemist and a great person, on the occasion of his 50th birthday.

† Author to whom correspondence should be addressed.

H_3BCO ,⁵ $\text{SnCl}_2(\text{CO})$,⁶ $\text{PbX}_2(\text{CO})$ ($\text{X} = \text{F}, \text{Cl}, \text{Br}, \text{I}$),⁶ $\text{Au}(\text{CO})\text{Cl}$,⁷ and $[\text{Tp}^{\text{R,R}}]\text{Cu}(\text{CO})$.⁸⁻¹⁰ More recently, homoleptic carbonyl complexes of the noble metals have been synthesized.¹¹ Specific examples include the complexes $[\text{Ag}(\text{CO})][\text{B}(\text{OTeF}_5)_4]$,¹² $[\text{Ag}(\text{CO})_2][\text{B}(\text{OTeF}_5)_4]$,¹³ $[\text{Au}(\text{CO})][\text{SO}_3\text{F}]$,¹⁴ $[\text{Au}(\text{CO})_2][\text{UF}_6]$,¹⁵ $[\text{Au}(\text{CO})_2][\text{Sb}_2\text{F}_{11}]$,¹⁶ $[\text{Hg}(\text{CO})_2][\text{Sb}_2\text{F}_{11}]_2$,¹⁷ and $[\text{Hg}_2(\text{CO})_2][\text{Sb}_2\text{F}_{11}]_2$,¹⁷ synthesized independently by the research groups of Strauss, Willner and Aubke, and Adelmhelm. In addition to these carbonyl complexes, there also exists a small, but growing, number of carbonyl complexes of the transition metals in which $d \rightarrow \pi^*$ back-bonding must also be considered as weak. Such complexes may be regarded as non-classical in the sense that the bonding differs significantly from that in traditional metal carbonyl complexes, for which $d \rightarrow \pi^*$ back-bonding provides an important contribution. In particular, transition metal centers that are formally d^0 are expected to bind CO in a non-classical fashion,^{18,19} and the first such zirconium carbonyl complex, namely thermally unstable $\text{Cp}_2^*\text{ZrH}_2(\text{CO})$, was observed by Bercaw in 1976 using low temperature ^1H NMR spectroscopy.^{20,21} However, since Bercaw's discovery of $\text{Cp}_2^*\text{ZrH}_2(\text{CO})$, there had been relatively few advances in this area until 1994, when the non-classical zirconium carbonyl complexes $[(\eta^5\text{-C}_5\text{R}_5)_2\text{Zr}(\eta^2\text{-COCH}_3)(\text{CO})]^+$ ($\text{R} = \text{H}, \text{Me}$) and $[\text{Cp}_2^*\text{Zr}(\eta^3\text{-C}_3\text{H}_5)(\text{CO})]^+$ were isolated by Jordan^{22,23} and Stryker,²⁴ respectively.^{25,26} In this paper, we report the syntheses, characterization, and reactivities of the non-classical zirconium carbonyl complexes $\text{Cp}_2^*\text{Zr}(\eta^2\text{-E}_2)(\text{CO})$ ($\text{E} = \text{S}, \text{Se}, \text{Te}$).

RESULTS AND DISCUSSION

We have recently reported the syntheses and structures of some terminal chalcogenido complexes of zirconium and hafnium, namely $\text{Cp}_2^*\text{M}(\text{E})(\text{NC}_5\text{H}_5)$ ($\text{Cp}^\dagger = \text{Cp}^*$ or $\text{Cp}^{\text{Et}*}$; $\text{M} = \text{Zr},^{27} \text{Hf}$; $^{28} \text{E} = \text{O}, \text{S}, \text{Se}, \text{Te}$).²⁹ With the exception of the hafnium oxo derivatives $\text{Cp}_2^*\text{Hf}(\text{O})(\text{NC}_5\text{H}_5)$,³⁰ the terminal chalcogenido complexes are all prepared by the reactions of the dicarbonyl complexes $\text{Cp}_2^*\text{M}(\text{CO})_2$ with either N_2O , S, Se, or Te, in the presence of pyridine (eq. (1)).



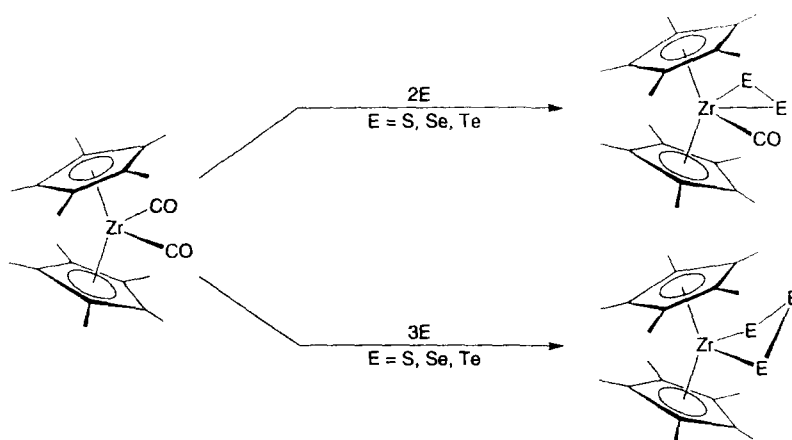
As also observed by Bergman for the syntheses of $\text{Cp}_2^*\text{Zr}(\text{S})(\text{NC}_5\text{H}_5)$ and $\text{Cp}_2^*\text{Zr}(\text{S})(\text{NC}_5\text{H}_4\text{Bu}^t)$,³¹

and by Andersen for the syntheses of $\text{Cp}_2^*\text{Ti}(\text{O})(\text{NC}_5\text{H}_5)$ and $\text{Cp}_2^*\text{Ti}(\text{O})(\text{NC}_5\text{H}_4\text{Ph})$,³² pyridine and its derivatives evidently provide an important role in stabilizing the multiply bonded $[\text{Cp}_2^*\text{M}(\text{E})]$ moiety. In order to provide more information concerning the formation of the terminal chalcogenido moieties by oxidation of the dicarbonyl complexes, we have investigated the reactions of $\text{Cp}_2^*\text{Zr}(\text{CO})_2$ with N_2O , S, Se, and Te in the absence of pyridine. The results of these studies include (i) the syntheses of the non-classical zirconium carbonyl complexes $\text{Cp}_2^*\text{Zr}(\eta^2\text{-E}_2)(\text{CO})$ ($\text{E} = \text{S}, \text{Se}, \text{Te}$), and (ii) the structural determination of the ditellurido derivative $\text{Cp}_2^*\text{Zr}(\eta^2\text{-Te}_2)(\text{CO})$, which exists in both triclinic and tetragonal modifications. The tetragonal version of $\text{Cp}_2^*\text{Zr}(\eta^2\text{-Te}_2)(\text{CO})$ provides an interesting example of crystallographic disorder which results in the derivation of an incorrect Zr—C bond length, and yet a correct C—O bond length.

Reactions of $\text{Cp}_2^\text{Zr}(\text{CO})_2$ with two equivalents of S, Se, and Te: syntheses of $\text{Cp}_2^*\text{Zr}(\eta^2\text{-E}_2)(\text{CO})$*

In the absence of pyridine, the dicarbonyl complex $\text{Cp}_2^*\text{Zr}(\text{CO})_2$ reacts with the elemental chalcogens E ($\text{E} = \text{S}, \text{Se}, \text{and Te}$) at *ca.* 80–90°C to give the dichalcogenido and trichalcogenido complexes, $\text{Cp}_2^*\text{Zr}(\eta^2\text{-E}_2)(\text{CO})$ and $\text{Cp}_2^*\text{Zr}(\eta^2\text{-E}_3)$ (Scheme 1).³³ The dichalcogenido-carbonyl complexes $\text{Cp}_2^*\text{Zr}(\eta^2\text{-E}_2)(\text{CO})$ may be readily isolated in *ca.* 50–55% yield by performing the reactions under conditions in which the chalcogen is used as the limiting reagent in order to minimize the quantity of $\text{Cp}_2^*\text{Zr}(\eta^2\text{-E}_3)$ in the final product mixture.³⁴ The excess $\text{Cp}_2^*\text{Zr}(\text{CO})_2$ is readily removed by washing with pentane. $\text{Cp}_2^*\text{Zr}(\text{CO})_2$ also reacts with excess N_2O at *ca.* 80°C,³⁵ but in contrast to the reactions with S, Se, and Te, this reaction results in significant decomposition.³⁶

The complexes $\text{Cp}_2^*\text{Zr}(\eta^2\text{-E}_2)(\text{CO})$ are of primary interest because they represent rare examples of non-classical transition metal carbonyl complexes. Since non-classical carbonyl complexes may be expected to play important roles in the functionalization of CO by d^0 transition metal centers (e.g. CO insertion into metal-hydride and metal-alkyl bonds),³⁷ the nature of the zirconium-carbonyl interaction in the complexes $\text{Cp}_2^*\text{Zr}(\eta^2\text{-E}_2)(\text{CO})$ is of considerable interest. The ν_{CO} stretching frequencies are of central importance for characterizing the zirconium-carbonyl interaction and are listed in Table 1, together with the values for the isotopically ^{13}C -labeled derivatives $\text{Cp}_2^*\text{Zr}(\eta^2\text{-E}_2)(^{13}\text{CO})$, which exhibit the expected isotope shifts ($\nu_{^{12}\text{CO}}/\nu_{^{13}\text{CO}} = 1.023$).



Scheme 1.

Table 1. ν_{CO} Stretching frequencies for $\text{Cp}_2^*\text{Zr}(\eta^2\text{-E}_2)(\text{CO})$

	$\nu_{12\text{CO}}$ (cm^{-1})	$\nu_{13\text{CO}}$ (cm^{-1})	$\nu_{12\text{CO}}/\nu_{13\text{CO}}^a$
$\text{Cp}_2^*\text{Zr}(\eta^2\text{-S}_2)(\text{CO})$	2057	2011	1.023
$\text{Cp}_2^*\text{Zr}(\eta^2\text{-Se}_2)(\text{CO})$	2037	1991	1.023
$\text{Cp}_2^*\text{Zr}(\eta^2\text{-Te}_2)(\text{CO})$	2006	1961	1.023

^a Calculated $\nu_{12\text{CO}}/\nu_{13\text{CO}} = 1.023$.

In the absence of back-bonding, the ν_{CO} stretching frequency for a metal–carbonyl derivative would be expected to be higher than the value for free CO (2143 cm^{-1}).² The origin of this effect is the fact that the CO σ -donor orbital is weakly antibonding and removal of this electron density results in an increase in the strength of the C—O σ -interaction.³⁸ Indeed, in the gas phase, the CO stretching frequency of the cation $[\text{CO}]^+$ (2184 cm^{-1}) is higher than that in neutral CO (2143 cm^{-1}).² Furthermore, a theoretical study on the dissociation of a single carbonyl ligand from $\text{Cr}(\text{CO})_6$ has suggested that at long Cr—C distances the CO ligand behaves only as a σ -donor and that the C—O bond distance becomes shorter than the value in free CO.^{4a}

The ν_{CO} stretching frequencies of $\text{Cp}_2^*\text{Zr}(\eta^2\text{-E}_2)(\text{CO})$ span the range $2006\text{--}2057 \text{ cm}^{-1}$, with the disulfido and ditellurido derivatives having the higher and lower values, respectively.³⁹ However, even though the disulfido complex $\text{Cp}_2^*\text{Zr}(\eta^2\text{-S}_2)(\text{CO})$ exhibits the highest ν_{CO} stretching frequency for the neutral zirconocene derivatives of which we are aware (Table 2) it is less than that in free CO (2143 cm^{-1}). A similar observation was also made by Bercaw concerning $\text{Cp}_2^*\text{ZrH}_2(\text{CO})$,^{20,40} for which the ν_{CO} stretching fre-

quency of 2044 cm^{-1} is intermediate between that of $\text{Cp}_2^*\text{Zr}(\eta^2\text{-S}_2)(\text{CO})$ and $\text{Cp}_2^*\text{Zr}(\eta^2\text{-Te}_2)(\text{CO})$. Although these non-classical zirconium carbonyl complexes exhibit ν_{CO} stretching frequencies that are lower than in free CO, it is noteworthy that they are indeed greater than the corresponding values in the related d^2 complex $\text{Cp}_2^*\text{Zr}(\text{CO})_2$ (1945 and 1852 cm^{-1}).⁴¹ For $\text{Cp}_2^*\text{ZrH}_2(\text{CO})$, the lowering of the ν_{CO} stretching frequency with respect to carbon monoxide was proposed to arise from donation of electron density from a filled metal–hydride bonding orbital into an in-plane π^* CO orbital.⁴⁰ It is possible that a related effect may be one of the factors responsible for the lowering of the ν_{CO} stretching frequencies of the dichalcogenido complexes $\text{Cp}_2^*\text{Zr}(\eta^2\text{-E}_2)(\text{CO})$. In this regard, we note that the separation between the carbonyl carbon atom and the adjacent tellurium atom in $\text{Cp}_2^*\text{Zr}(\eta^2\text{-Te}_2)(\text{CO})$ is *ca.* 2.93 \AA (*vide infra*), a value that is intermediate between the sum of the single bond covalent radii (2.14 \AA) and the sum of their van der Waals radii (3.74 \AA).⁴²

For comparative purposes, the ν_{CO} stretching frequencies, summarized in Table 2, for some terminal zirconium carbonyl derivatives span the substantial range $1757\text{--}2176 \text{ cm}^{-1}$. It is noteworthy that, of these complexes, only Jordan's cationic *O-endo* isomers $[\text{Cp}_2^*\text{Zr}(\eta^2\text{-COCH}_3)(\text{CO})]^+$ (2152 cm^{-1}) and $[\text{Cp}_2^*\text{Zr}(\eta^2\text{-COCH}_3)(\text{CO})]^+$ (2176 cm^{-1})²² exhibit ν_{CO} stretching frequencies greater than that in free CO. However, since ν_{CO} stretching frequencies generally increase with the increasing positive charge on a complex,² such increases compared to the neutral non-classical zirconium carbonyl complexes are to be anticipated.⁴³ In this regard, it may be more appropriate to compare the ν_{CO} stretching frequencies of cationic carbonyl complexes with the value for the cation $(\text{CO})^+$ (2184 cm^{-1}), rather than

Table 2. ν_{CO} Stretching frequencies for some terminal zirconium carbonyl complexes

	$\nu_{(\text{CO})}$ (cm^{-1})	Ref.
<i>O-endo</i> -[Cp ₂ Zr(η^2 -COCH ₃)(CO)] ⁺	2176	22
<i>O-exo</i> -[Cp ₂ Zr(η^2 -COCH ₃)(CO)] ⁺	2123	22
<i>O-endo</i> -[Cp [*] Zr(η^2 -COCH ₃)(CO)] ⁺	2152	22
<i>O-exo</i> -[Cp [*] Zr(η^2 -COCH ₃)(CO)] ⁺	2105	22
[Cp ₂ Zr{ η^2 -CH(Me)(6-ethylpyrid-2-yl)-C,N}(CO)] ⁺	2095	23
[Cp [*] Zr(η^3 -C ₃ H ₅)(CO)] ⁺	2079	24
Cp [*] ₂ Zr(η^2 -S ₂)(CO)	2057	This work
Cp [*] ₂ ZrH ₂ (CO)	2044	40
Cp [*] ₂ Zr(η^2 -Se ₂)(CO)	2037	This work
Cp [*] ₂ Zr(η^2 -Te ₂)(CO)	2006	This work
(η^5 -2,4-C ₇ H ₁₁) ₂ Zr(CO) ₂	2000, 1942	84
(η^5 -C ₉ H ₇) ₂ Zr(CO) ₂	1985, 1899	85
Cp ₂ Zr(CO) ₂	1976, 1887	86
	1978, 1888	87
(η^5 -C ₅ H ₄ SiMe ₃) ₂ Zr(CO) ₂	1970, 1880	88
(η^5 -2,4-C ₇ H ₁₁) ₂ Zr(CO)	1968	84
[η^5 -C ₅ H ₃ (SiMe ₃) ₂] ₂ Zr(CO) ₂	1962, 1875	88
CpZr(CO) ₂ (dmpe)Cl	1955, 1885	89
Cp [*] ₂ Zr(CO) ₂	1945, 1852	41
Cp [*] ₂ Zr(CO)(η^2 -OCHCH ₂ CHMe ₂)	1940	55
[η^3 -MeC(CH ₂ PMe ₂) ₃] ₂ Zr(CO) ₄	1938, 1820	90
Cp ₂ Zr(CO)[CH{OZr(H)Cp [*] }]	1925	91
[Pr [*] ₄ N] ₂ [(Ph ₃ Sn) ₄ Zr(CO) ₄]	1886	92
Cp ₂ Zr(CO)(PMe ₃)	1852	93
Cp ₂ Zr(CO)[P(OMe) ₃]	1849	94
Cp ₂ Zr(CO)(PPh ₃)	1842	95
Cp ₂ Zr(CO)(PPh ₂ Me)	1840	96
Cp ₂ Zr(CO)(μ - η^1 , η^5 -C ₅ H ₄)Ru(CO) ₂	1840	97
Cp ₂ Zr(η^2 -Me ₂ SiNBu ^t)(CO)	1797	26
[CpZr(CO) ₄] ⁻	1923, 1781	98
[Cp [*] Zr(CO) ₄] ⁻	1916, 1781	99
[K(cryptand 2.2.2)] ₂ [Zr(CO) ₆]	1757	100

neutral CO (2143 cm^{-1}). Nevertheless, it does appear that all of the terminal carbonyl complexes in Table 2 which may be considered to be non-classical exhibit ν_{CO} stretching frequencies that are greater than 2000 cm^{-1} .

A notable exception, however, is that of Cp₂Zr(η^2 -Me₂SiNBu^t)(CO), which exhibits an extremely low ν_{CO} stretching frequency of 1797 cm^{-1} .²⁶ The X-ray structure of Cp₂Zr(η^2 -Me₂SiNBu^t)(CO) indicates that the C and Si atoms are separated by only *ca.* 2.4 Å, which, although greater than the sum of the single bond covalent radii (1.94 Å),⁴² is substantially less than the sum of the van der Waals radii (3.60 Å).⁴² It has been suggested that there is a direct σ - π^* interaction between Si and the CO ligand, which may thereby result in a lowering of the ν_{CO} stretching frequency. In support of this suggestion, the $J_{\text{Si-C}}$ coupling constant for the Si...CO interaction is 24 Hz, compared to the

value of 56 Hz for the direct one-bond Si—CH₃ interaction in this complex.

The [Zr—CO] moieties in Cp^{*}₂Zr(η^2 -E₂)(CO) are also characterized by ¹³C NMR chemical shifts in the range 219–232 ppm (Table 3), downfield from the value of 184.4 ppm for CO in C₆D₆.⁴⁴ It is noteworthy that there is also an empirical correlation of the ¹³C NMR chemical shifts with the

Table 3. ¹³C NMR data for Zr—CO groups of Cp^{*}₂Zr(η^2 -E₂)(CO)

	δ (ppm)
Cp [*] ₂ Zr(η^2 -S ₂)(CO)	218.5
Cp [*] ₂ Zr(η^2 -Se ₂)(CO)	222.5
Cp [*] ₂ Zr(η^2 -Te ₂)(CO)	231.8

ν_{CO} stretching frequencies, in which an increase in the ^{13}C NMR chemical shift is accompanied by a reduction of the ν_{CO} stretching frequency.^{45,46} The correlation also holds true for the structurally related complex $\text{Cp}_2\text{Zr}(\eta^2\text{-Me}_2\text{SiNBu}^t)(\text{CO})$, with a very low ν_{CO} stretching frequency of 1797 cm^{-1} and a large chemical shift of $\delta(\text{CO}) = 290.7\text{ ppm}$,²⁶ as illustrated in Fig. 1. For further comparison, the values for some other monocarbonyl zirconium complexes are also included in Fig. 1. The data for these zirconium carbonyl complexes indicate that there is a general decrease in the shielding of the carbon atom of the CO group as π -back-bonding becomes more significant. It is worthwhile to relate this correlation with that for the ^{13}C NMR chemical shifts of alkyne ligands, in which alkynes which donate only two-electrons to a metal center are shielded with respect to those which donate four-electrons.⁴⁷

The nature of the zirconium-carbonyl interaction has also been investigated by X-ray diffraction studies on the ditellurido derivative. $\text{Cp}_2^*\text{Zr}(\eta^2\text{-Te}_2)(\text{CO})$ exists in at least two crystalline modifications, namely triclinic $P\bar{1}$ (No. 2) and tetragonal $P4n2$ (No. 118). For reasons that will become apparent, we will discuss only the triclinic structure here, and leave discussion of the tetragonal version to later in the text. The asymmetric unit of the triclinic cell is composed of two crystallographically

independent, but similar, $\text{Cp}_2^*\text{Zr}(\eta^2\text{-Te}_2)(\text{CO})$ molecules. ORTEP drawings of one of the molecules are shown in Figs 2 and 3, and selected bond lengths and angles for both molecules are summarized in Table 4.

The average Zr—CO and C—O bond lengths are $2.241(7)\text{ \AA}$ and $1.123(9)\text{ \AA}$, respectively. For comparison, the corresponding values for other structurally characterized terminal zirconium carbonyl derivatives are listed in Table 5. The Zr—C and C—O bond lengths in these complexes span the ranges of $2.15\text{--}2.25\text{ \AA}$ and $1.12\text{--}1.16\text{ \AA}$, respectively. Although these ranges are relatively small compared with the large changes in ν_{CO} stretching frequency, it is evident that the zirconium-carbonyl interaction in $\text{Cp}_2^*\text{Zr}(\eta^2\text{-Te}_2)(\text{CO})$ is at an extreme that is best described as having a long Zr—C bond length and a short C—O bond length. In this regard, it is worthwhile to compare these metrical parameters with those of the related d^2 carbonyl complex $\text{Cp}_2^*\text{Zr}(\text{CO})_2$,⁴¹ for which the bond lengths $d(\text{Zr—CO}) = 2.145(9)\text{ \AA}$ and $d(\text{C—O}) = 1.16(1)\text{ \AA}$ are best represented at the opposite extreme. Thus, $\text{Cp}_2^*\text{Zr}(\text{CO})_2$ may be regarded as having short Zr—CO and long C—O bond lengths, indicative of substantial $d \rightarrow \pi^*$ back-bonding and in accord with the lower ν_{CO} stretching frequencies. $\text{Cp}_2^*\text{Zr}(\text{CO})_2$ and $\text{Cp}_2^*\text{Zr}(\eta^2\text{-E}_2)(\text{CO})$ thereby provide illustrative examples of the different physical

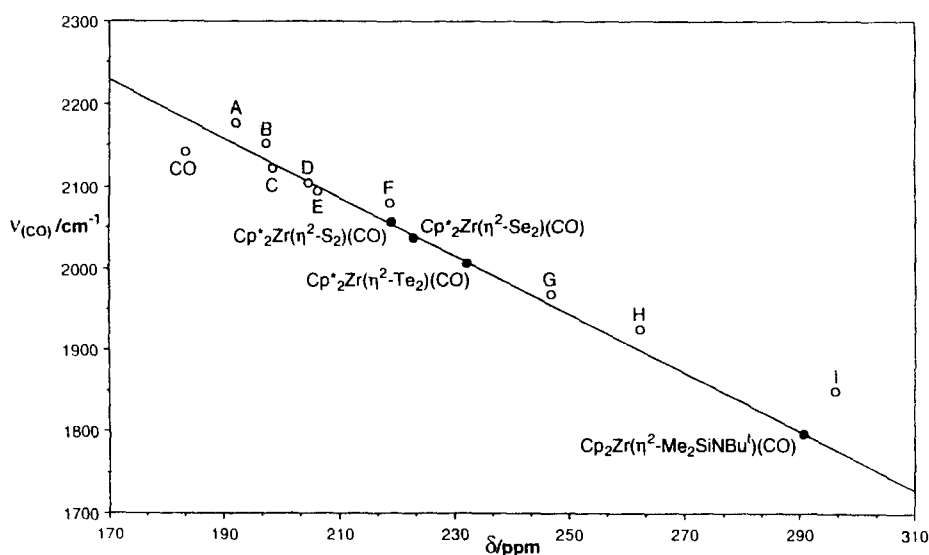


Fig. 1. Correlation of ν_{CO} stretching frequencies and ^{13}C NMR shifts for some zirconium carbonyl complexes. The straight line is drawn through the points for $\text{Cp}_2^*\text{Zr}(\eta^2\text{-E}_2)(\text{CO})$ ($\text{E} = \text{S}, \text{Se}, \text{Te}$) and $\text{Cp}_2\text{Zr}(\eta^2\text{-Me}_2\text{SiNBu}^t)(\text{CO})$. (A) *O-endo*- $[\text{Cp}_2\text{Zr}(\eta^2\text{-COCH}_3)(\text{CO})]^+$, (B) *O-endo*- $[\text{Cp}^*_2\text{Zr}(\eta^2\text{-COCH}_3)(\text{CO})]^+$, (C) *O-exo*- $[\text{Cp}_2\text{Zr}(\eta^2\text{-COCH}_3)(\text{CO})]^+$, (D) *O-exo*- $[\text{Cp}^*_2\text{Zr}(\eta^2\text{-COCH}_3)(\text{CO})]^+$, (E) $[\text{Cp}_2\text{Zr}\{\eta^2\text{-CH}(\text{Me})(6\text{-ethylpyrid-2-yl})\text{-C,N}\}(\text{CO})]^+$, (F) $[\text{Cp}^*_2\text{Zr}(\eta^2\text{-C}_3\text{H}_5)(\text{CO})]^+$, (G) $(\eta^5\text{-2,4-C}_7\text{H}_{11})_2\text{Zr}(\text{CO})$, (H) $\text{Cp}_2\text{Zr}(\text{CO})[\text{CH}\{\text{OZr}(\text{H})\text{Cp}^*_2\}]$, (I) $\text{Cp}_2\text{Zr}(\text{CO})[\text{P}(\text{OMe})_3]$. See Table 2 for literature references.

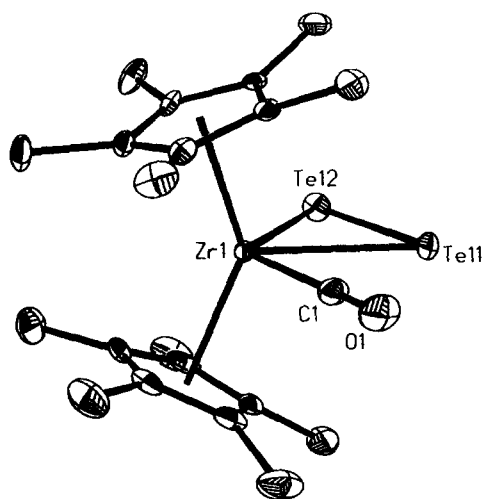


Fig. 2. ORTEP drawing for one of the molecules of the triclinic modification of $\text{Cp}_2^*\text{Zr}(\eta^2\text{-Te}_2)(\text{CO})$.

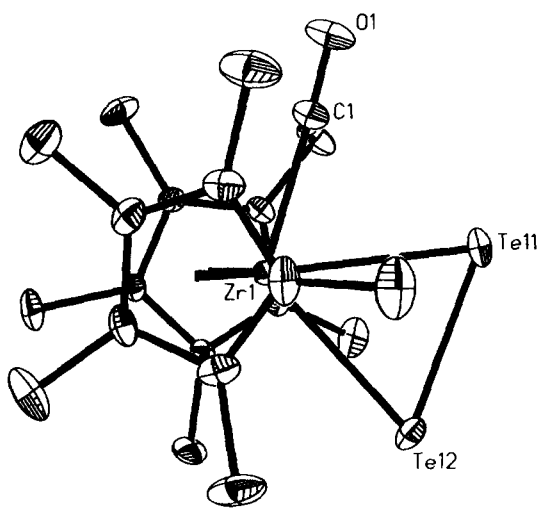


Fig. 3. ORTEP drawing for one of the molecules of the triclinic modification of $\text{Cp}_2^*\text{Zr}(\eta^2\text{-Te}_2)(\text{CO})$.

properties that are to be expected for classical and non-classical transition metal–carbonyl complexes, respectively.

In addition to issues pertaining to the nature of the zirconium–carbonyl interaction, the complexes $\text{Cp}_2^*\text{Zr}(\eta^2\text{-E}_2)(\text{CO})$ are also of interest since mononuclear η^2 -dichalcogenido complexes are not common. Indeed, for Ti, Zr, and Hf, the only structurally characterized examples of which we are aware are disulfido $[\text{L}_n\text{Ti}(\eta^2\text{-S}_2)]^{48}$ and peroxy $[\text{L}_n\text{Ti}(\eta^2\text{-O}_2)]^{49}$ derivatives of titanium. Moreover, structurally characterized mononuclear η^2 -ditellurido complexes of the transition metals are particularly rare, as summarized in Table 6.⁵⁰

The $[\text{Zr}(\eta^2\text{-Te}_2)]$ moiety is characterized by average Zr–Te and Te–Te bond lengths of 2.96(1) and 2.69(2) Å, respectively. The Te–Te bond length of 2.69(2) Å in $\text{Cp}_2^*\text{Zr}(\eta^2\text{-Te}_2)(\text{CO})$ is close to the value that would be anticipated for a single bond. For example, the Te–Te single bond length that would be predicted by twice the covalent radius of Te is 2.74 Å,⁴² while the Te–Te single bond length in the tritellurido complex $\text{Cp}_2^*\text{Zr}(\eta^2\text{-Te}_3)$ is 2.72(1) Å (*vide infra*). Comparable Te–Te bond lengths are observed for other mononuclear ditellurido complexes (Table 6), and also diarylditellurides, e.g. Ph_2Te_2 [2.712(2) Å],⁵¹ and (*p*-tolyl)₂Te₂ [2.697(3) Å].^{52,53} The average Zr–Te bond length [2.96(1) Å] in $\text{Cp}_2^*\text{Zr}(\eta^2\text{-Te}_2)(\text{CO})$ is slightly longer than would be predicted by (i) the sum of the covalent radii of Zr and Te (2.88 Å),⁴² and (ii) Zr–Te single bond lengths that have been measured for other zirconocene derivatives (2.85–2.89 Å), as listed in Table 7.

The bonding within the $[\text{Zr}(\eta^2\text{-E}_2)]$ moiety may be described by a combination of the two resonance structures shown in Fig. 4, analogous to the metallacyclopropane/metal–olefin dichotomy.⁵⁴ On the basis that the observed Zr–Te and Te–Te bond lengths are close to the values expected for single bonds, the $[\text{Zr}(\eta^2\text{-Te}_2)]$ interaction would be better represented as resonance structure (A). However,

Table 4. Selected bond lengths (Å) and angles (°) for $\text{Cp}_2^*\text{Zr}(\eta^2\text{-Te}_2)(\text{CO})$

Zr(1)—Te(11)	2.972(1)	Zr(2)—Te(21)	2.956(1)
Zr(1)—Te(12)	2.952(1)	Zr(2)—Te(22)	2.961(1)
Zr(1)—C(1)	2.247(7)	Zr(2)—C(2)	2.234(6)
C(1)—O(1)	1.122(9)	C(2)—O(2)	1.124(8)
Te(11)—Te(12)	2.688(1)	Te(21)—Te(22)	2.692(1)
Te(11)—Zr(1)—Te(12)	54.0(1)	Te(21)—Zr(2)—Te(22)	54.1(1)
Te(12)—Te(11)—Zr(1)	62.6(1)	Te(22)—Te(21)—Zr(2)	63.0(1)
Zr(1)—Te(12)—Te(11)	63.4(1)	Zr(2)—Te(22)—Te(21)	62.9(1)
Zr(1)—C(1)—O(1)	177.2(8)	Zr(2)—C(2)—O(2)	177.3(8)
C(1)—Zr(1)—Te(11)	66.5(2)	C(2)—Zr(2)—Te(22)	66.8(2)

Table 5. Zr—C and C—O bond lengths for some terminal zirconium carbonyl complexes

	$d(\text{Zr—CO})$ (Å)	$d(\text{C—O})$ (Å)	Ref.
<i>O-exo</i> -[Cp ₂ *Zr(η ² -COCH ₃)(CO)] ⁺	2.25(1)	1.13(1)	22
Cp ₂ *Zr(η ² -Te ₂)(CO)	2.241(7)	1.123(9)	This work
Cp ₂ Zr(CO) ₂	2.187(4)	—	101
Cp ₂ Zr(CO)[P(OMe) ₃]	2.160(7)	1.157(8)	94
Cp ₂ *Zr(CO) ₂	2.145(9)	1.16(1)	41
Cp ₂ Zr(η ² -Me ₃ SiNBu ^t)(CO)	2.145(5)	1.162(7)	26
CpZr(CO) ₂ (dmpe)Cl	2.220(2)	1.142(10)	89
Cp ₂ Zr(CO)(μ-η ¹ ,η ² -C ₅ H ₄)Ru(CO) ₂	2.240(6)	1.150(7)	97
(η ⁵ -C ₅ H ₇) ₂ Zr(CO) ₂	2.20(2)	1.130(8)	85
(η ⁵ -2,4-C ₇ H ₁₁) ₂ Zr(CO) ₂	2.208(5)	1.142(5)	84
(η ⁵ -2,4-C ₇ H ₁₁) ₂ Zr(CO)	2.164(8)	1.153(8)	84
[η ³ -MeC(CH ₂ PMe ₂) ₃]Zr(CO) ₄	2.17(4)	1.16(3)	90
[K(cryptand 2.2.2)] ₂ [Zr(CO) ₆]	2.210(4)	1.162(5)	100
[Pr ^{IV} N] ₂ [(Ph ₃ Sn) ₄ Zr(CO) ₄]	2.232(5)	1.155(6)	92

Table 6. Te—Te bond lengths in mononuclear η²-ditellurido complexes

	$d(\text{Te—Te})$ (Å)	Ref.
Cp ₂ *Zr(η ² -Te ₂)(CO)	2.69(2) ^a	This work
W(PMe ₃)(CNBu ^t) ₄ (η ² -Te ₂)	2.680(2)	102
Cp ₂ *Ta(η ² -Te ₂)H	2.678(2) ^b	103
{η ³ -PhP(CH ₂ CH ₂ PPh ₂) ₂ }Ni(η ² -Te ₂)	2.668(1)	104
{η ³ -MeC(CH ₂ PPh ₂) ₃ }Ni(η ² -Te ₂)	2.665(2)	104

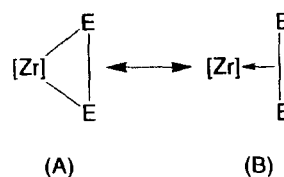
^a Average value for two independent molecules.

^b Cp₂*Ta(η²-Te₂)H is disordered about a crystallographic two-fold axis, so that the derived bond length may not be accurate.

Table 7. Zr—Te single bond lengths in zirconocene derivatives

	$d(\text{Zr—Te})$ (Å)	Ref.
Cp ₂ *Zr(η ² -Te ₂)(CO)	2.96(1)	This work
Cp ₂ *Zr(η ² -Te ₃)	2.89(1)	This work
[(η ⁵ -C ₅ H ₄ Bu ^t) ₂ Zr(Te) ₂]	2.85(1)	105
[(η ⁵ -C ₅ H ₄ Bu ^t) ₂ Zr] ₂ (Te)(O)	2.88(1)	106

since the average Zr—Te bond length in Cp₂*Zr(η²-Te₂)(CO) (2.96(1) Å) is marginally longer than that in Cp₂*Zr(η²-Te₃) (2.89(1) Å), a contribution from resonance structure (B) should not be neglected. On balance, however, it would appear that the more appropriate formal descrip-

Fig. 4. Resonance structures for the [Zr(η²-Te₂)] interaction.

tion for Cp₂*Zr(η²-Te₂)(CO) is a Zr^{IV} *d*⁰ complex, rather than the Zr^{III} *d*² alternative. Since the sulfido and selenido complexes Cp₂*Zr(η²-E₂)(CO) exhibit higher ν_{CO} stretching frequencies than that of the tellurido derivative, these complexes are also proposed to be more appropriately described as Zr^{IV} *d*⁰ complexes. In support of the above proposal, it is noteworthy that the carbonyl complex Cp₂*Zr(CO)(η²-OCHCH₂CHMe₂) exhibits the relatively low ν_{CO} stretching frequency of 1940 cm⁻¹, an observation that was attributed to a substantial contribution from the Zr^{III}-aldehyde resonance form.⁵⁵

*Reactions of Cp₂*Zr(CO)₂ with three equivalents of S, Se, and Te: syntheses of Cp₂*Zr(η²-E₃).*

Whereas the dichalcogenido carbonyl complexes Cp₂*Zr(η²-E₂)(CO) are obtained from the reactions between Cp₂*Zr(CO)₂ and *ca.* two equivalents of E (E = S, Se, Te), the corresponding reactions with three equivalents of chalcogen cleanly give the trichalcogenido complexes Cp₂*Zr(η²-E₃) (E = S, Se, Te), as shown in Scheme 1.

The sulfido derivative Cp₂*Zr(η²-S₃) was first iso-

lated by Shaver as a product of the reaction of $\text{Cp}_2^*\text{ZrCl}_2$ with Li_2S_x (generated in situ by the reaction of LiEt_3BH_x with S).⁵⁶ More recently, $\text{Cp}_2^*\text{Zr}(\eta^2\text{-S}_3)$ has also been prepared by the reaction of $\text{Cp}_2^*\text{Zr}(\text{SH})_2$ with elemental sulfur.^{57,58} It has also been reported that $\text{Cp}_2^*\text{Zr}(\eta^2\text{-S}_3)$ is formed by the reaction of $\text{Cp}_2^*\text{Zr}(\text{SH})_2$ with H_2S at 80°C ;⁵⁷ however, in our experience, $\text{Cp}_2^*\text{Zr}(\text{SH})_2$ is stable under such conditions.⁵⁹

The molecular structures of the trichalcogenido complexes $\text{Cp}_2^*\text{Zr}(\eta^2\text{-E}_3)$ ($\text{E} = \text{S}, \text{Se}, \text{Te}$) have been determined by X-ray diffraction, as shown in Figs 5–7. Selected bond lengths and angles are presented in Table 8. The structures of $\text{Cp}_2^*\text{Zr}(\eta^2\text{-E}_3)$ are similar to that of the titanium analogue $\text{Cp}_2^*\text{Ti}(\eta^2\text{-S}_3)$,^{60,61} and each contain a puckered four-membered $[\text{ME}_3]$ ring. The Zr—E bond lengths are

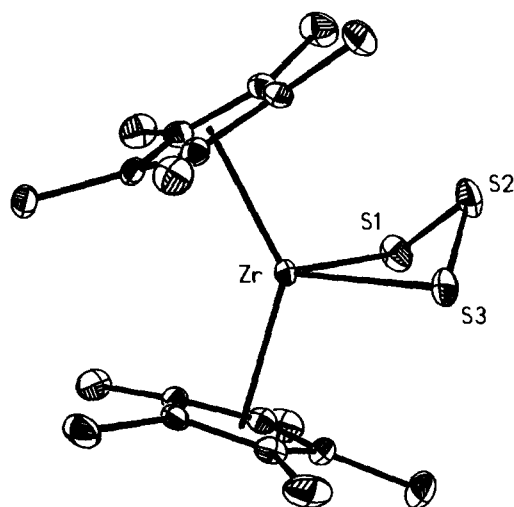


Fig. 5. ORTEP drawing for $\text{Cp}_2^*\text{Zr}(\eta^2\text{-S}_3)$.

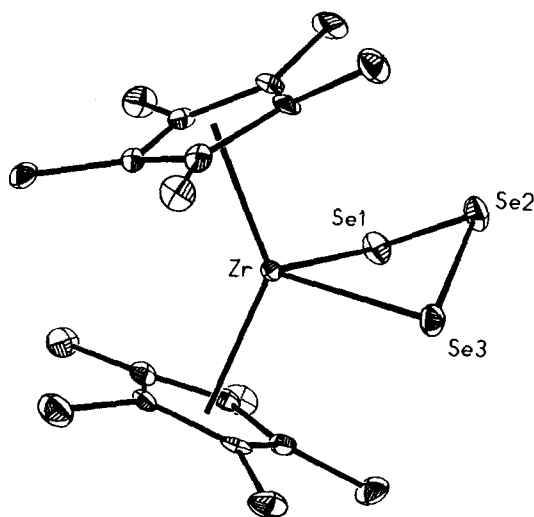


Fig. 6. ORTEP drawing for $\text{Cp}_2^*\text{Zr}(\eta^2\text{-Se}_3)$.

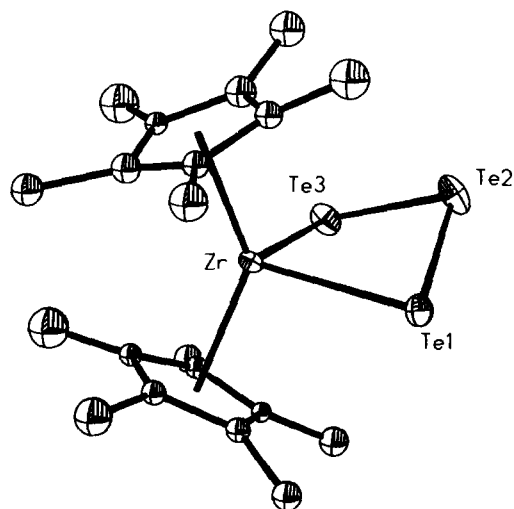


Fig. 7. ORTEP drawing for $\text{Cp}_2^*\text{Zr}(\eta^2\text{-Te}_3)$.

Table 8. Selected metrical data (in ångströms and in degrees) for $\text{Cp}_2^*\text{Zr}(\eta^2\text{-E}_3)$

	S	Se	Te ^a
Zr—C _{av}	2.56(5)	2.57(6)	2.57(8)
Zr—E _{av}	2.521(1)	2.653(3)	2.89(2)
Zr···E ^b	2.778(1)	3.033(1)	3.46(3)
$\Delta(\text{Zr—E})^c$	0.26	0.38	0.57
E—E _{av}	2.066(8)	2.337(3)	2.72(1)
$\Sigma_{\text{cov rad}}^d$	2.55	2.68	2.88
$\Sigma_{\text{van der Waals}}^d$	4.15	4.28	4.48
E—Zr—E	83.1(1)	88.2(1)	93.4(3)
Zr—E—E	73.8(1)	74.6(1)	76.2(9)
E—E—E	108.1(1)	104.5(1)	101.4(5)
Fold angle ^e	54	50	42

^a Average values for two independent molecules.

^b Zr···E is the distance between Zr and the central chalcogen of the $[\text{ZrE}_3]$ ring.

^c $\Delta(\text{Zr—E})$ is defined as the difference between the secondary Zr···E and primary Zr—E_{av} bond lengths.

^d See ref. 42.

^e The fold angle is defined as the angle between the E—Zr—E and E—E—E planes.

close to the sum of the single bond covalent radii of Zr and E⁴² (Table 8), while the distances between the zirconium center and the central chalcogens (Zr···E), which are substantially less than the sum of their van der Waals radii, are such that they may represent a weak secondary donor interaction. For example, the difference in Zr—S bond lengths for the central and lateral sulfur atoms, $\Delta(\text{Zr—E})$, is only 0.26 Å. The principal structural change that is observed for the complexes $\text{Cp}_2^*\text{Zr}(\eta^2\text{-E}_3)$ is a reduction in the puckering of the four-membered

ME₃ ring across the series S > Se > Te. Thus, the fold angle (defined as the angle between the E—Zr—E and E—E—E planes) decreases from 54° for the sulfido derivative to 42° for the tellurido derivative. These changes are also accompanied by (i) an increase in the magnitude of Δ(Zr—E), (ii) an increase in the E—Zr—E bond angle, and (iii) a decrease in the E—E—E bond angle (see Table 8).

It is noteworthy that the reactions between Cp₂Zr(CO)₂ and excess chalcogen give only the trichalcogenido derivatives, with no evidence for the formation of pentachalcogenido complexes Cp₂Zr(η²-E₅) which may have been anticipated by analogy with the cyclopentadienyl system. For example, the pentachalcogenido complexes Cp₂Zr(η²-S₅) and Cp₂Zr(η²-Se₅) have been prepared by the reactions of Cp₂ZrCl₂ with Li₂S_x and Li₂Se_x, respectively.^{56,62} In this regard, Shaver has made the general observation that for the titanium, zirconium, and hafnium sulfido systems, the natural ring size is six for the [Cp₂M] system, and four for the permethylated [Cp₂⁺M] system.⁵⁶ The structural characterization of Cp₂Zr(η²-E₃) (E = S, Se, Te) serves to suggest that the natural ring size is also four for [Cp₂⁺Zr] derivatives of the heavier chalcogens, Se and Te.

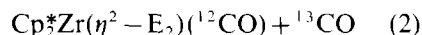
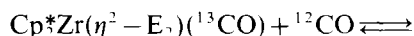
The molecular structures of the pentachalcogenido complexes Cp₂Zr(η²-S₅)⁶³ and Cp₂Zr(η²-Se₅)⁶² have been previously determined by X-ray diffraction.⁶⁴ The Zr—E bond lengths in these complexes are also similar to the respective values in the four-membered ring analogues, Cp₂Zr(η²-E₃). For comparison, the average Zr—E bond lengths for Cp₂Zr(η²-E₃) and Cp₂Zr(η²-E₅) are summarized in Table 9. Furthermore, these values are also similar to the average Zr—S (2.52 Å) and Zr—Se (2.66 Å) bond lengths for a series of Cp₂Zr(EX)Y complexes.^{27b}

The triselenido and tritellurido complexes Cp₂Zr(η²-E₃) have also been studied by ⁷⁷Se and ¹²⁵Te NMR spectroscopy. The triselenido complex exhibits two resonances at 136 and 555 ppm in the ⁷⁷Se NMR spectrum (Fig. 8). Each resonance exhibits Se satellites with ¹J_{77Se-77Se} = 184 Hz, simi-

lar to the value of 262 Hz for the anion Se₃²⁻.⁶⁵ On the basis of the relative intensities of the satellites, the resonance at 136 ppm is assigned to the central selenium, with the resonance at 555 ppm assigned to the metal-bound selenium atoms.⁶⁶ Studies on Cp₂Ti(η²-Se₅) have also demonstrated that the metal-bound selenium nuclei resonate to lower field than do the other selenium nuclei.^{67,68} Similar to the triselenido complex, the tritellurido derivative Cp₂Zr(η²-Te₃) also exhibits two resonances at 297 and -401 ppm in the ¹²⁵Te NMR spectrum, attributable to the Zr—Te and Te—Te—Te moieties, respectively. Furthermore, each resonance exhibits satellites with ¹J_{125Te-125Te} = 1800 Hz, of similar magnitude to the value of 2175 Hz observed for Te₃²⁻.⁶⁵

Reactivity of Cp₂Zr(η²-E₂)(CO) and Cp₂Zr(η²-E₃)

The carbonyl ligands of Cp₂Zr(η²-E₂)(CO) (E = S, Se, and Te) are labile, evidence for which is provided by ¹³C isotopic exchange studies. Thus, addition of excess ¹²CO to solutions of the ¹³C labeled derivatives Cp₂Zr(η²-E₂)(¹³CO) results in the formation of the isotopomer Cp₂Zr(η²-E₂)(¹²CO) (eq. (2)), as judged by the reduction in intensity of the ¹³C NMR signal that is attributable to the [Zr—¹³CO] moiety.



Furthermore, dynamic ¹³C NMR studies have demonstrated that the qualitative rates of CO exchange for the disulfido and diselenido complexes Cp₂Zr(η²-E₂)(CO) are substantially greater than for the ditellurido derivative, *i.e.* *k*_{Te} << *k*_{Se} ≈ *k*_{S}. Thus, upon exposure of the ¹³C-labeled disulfido and diselenido complexes Cp₂Zr(η²-E₂)(¹³CO) to ¹³CO, the resonances attributable to the [Zr—¹³CO] moiety are broadened considerably, indicative of rapid exchange on the NMR timescale.⁶⁹ In contrast, the corresponding Cp₂Zr(η²-Te₂)(¹³CO) derivative shows little broadening in the presence of ¹³CO. For example, the ¹³C NMR spectra for the diselenido and ditellurido derivatives Cp₂Zr(η²-E₂)(¹³CO) in the presence of the same concentration of ¹³CO are shown in Fig. 9, which also includes for reference the spectra of Cp₂Zr(η²-E₂)(¹³CO) in the absence of ¹³CO.}

The observation of slower CO exchange for the ditellurido complex, compared to the sulfido and selenido analogues, is in accord with the lower *v*_{CO} stretching frequency for this derivative. Specifically, the lower *v*_{CO} stretching frequency for Cp₂Zr(η²-Te₂)(CO) is indicative of greater back-

Table 9. Comparison of Zr—E bond lengths (Å) in Cp₂Zr(η²-E₃) and Cp₂Zr(η²-E₅) derivatives

	S	Se
Cp ₂ Zr(η ² -E ₃)	2.521(1)	2.653(3)
Cp ₂ Zr(η ² -E ₅)	2.535(9) ^a	2.657(3) ^b

^a Ref. 63.

^b Ref. 62.

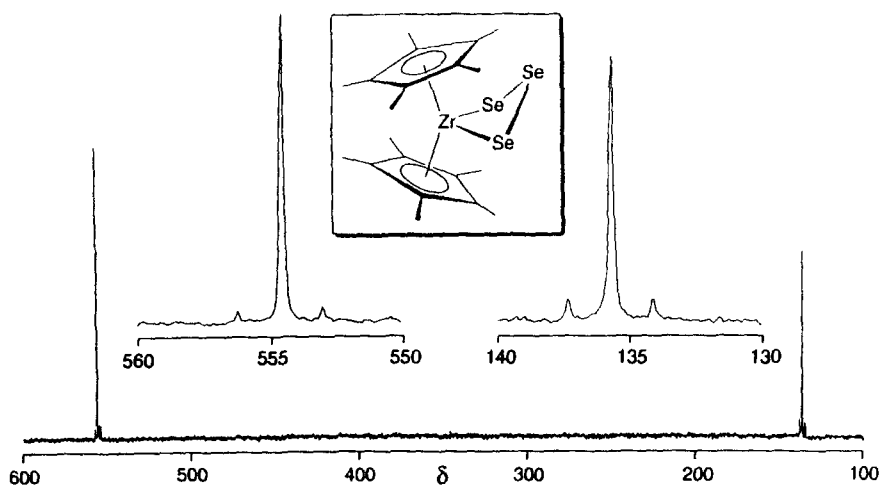


Fig. 8. $^{77}\text{Se}\{^1\text{H}\}$ NMR spectrum of $\text{Cp}^*_2\text{Zr}(\eta^2\text{-Se}_3)$.

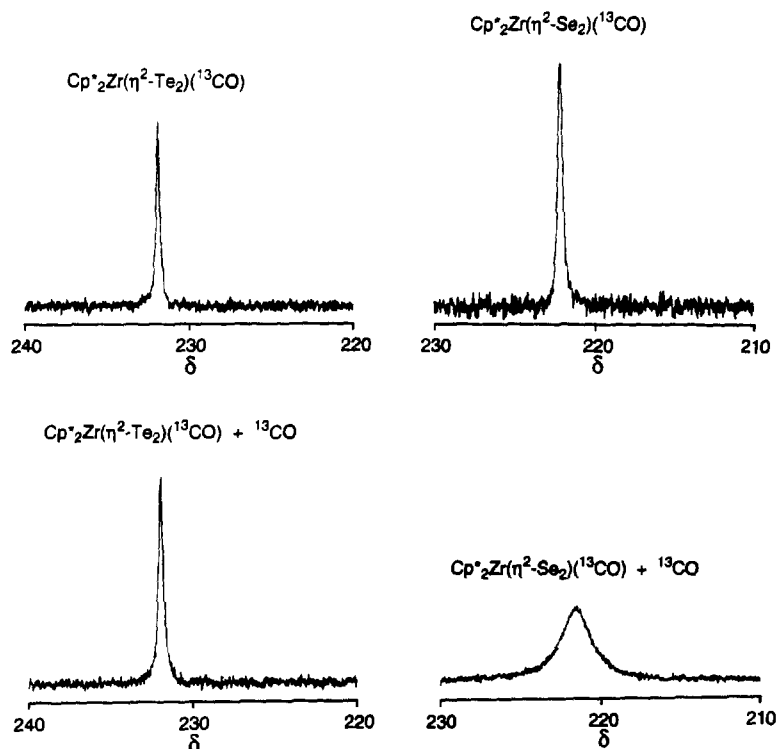
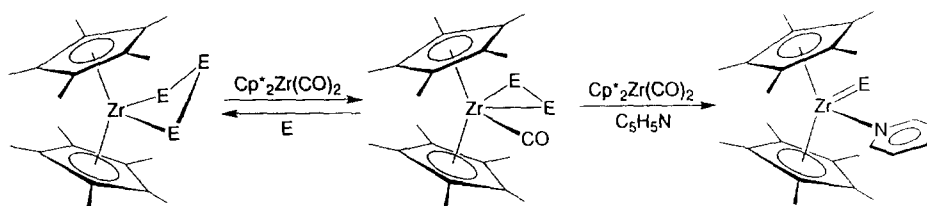


Fig. 9. ^{13}C NMR spectra of the CO region of $\text{Cp}^*_2\text{Zr}(\eta^2\text{-E}_2)(^{13}\text{CO})$ ($\text{E} = \text{Se}, \text{Te}$) in the absence and presence of ^{13}CO .

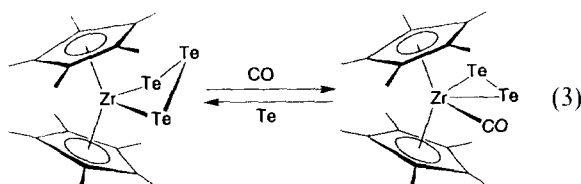
bonding, and therefore presumably a stronger zirconium–carbonyl interaction.⁷⁰

The dichalcogenido moieties in $\text{Cp}^*_2\text{Zr}(\eta^2\text{-E}_2)(\text{CO})$ are reactive towards a number of reagents. For example, one of the chalcogen atoms may be abstracted by $\text{Cp}^*_2\text{Zr}(\text{CO})_2$ in the presence of pyridine to give the terminal chalcogenido complexes $\text{Cp}^*_2\text{Zr}(\text{E})(\text{NC}_5\text{H}_5)$ (Scheme 2).⁷¹ The formation of $\text{Cp}^*_2\text{Zr}(\text{E})(\text{NC}_5\text{H}_5)$ in these reactions indicates that the dichalcogenido–car-

bonyl complexes $\text{Cp}^*_2\text{Zr}(\eta^2\text{-E}_2)(\text{CO})$ are viable intermediates in the syntheses of the terminal chalcogenido derivatives $\text{Cp}^*_2\text{Zr}(\text{E})(\text{NC}_5\text{H}_5)$ by the oxidation of $\text{Cp}^*_2\text{Zr}(\text{CO})_2$ with the elemental chalcogen in the presence of pyridine.^{27b} However, although consistent with the intermediacy of $\text{Cp}^*_2\text{Zr}(\eta^2\text{-E}_2)(\text{CO})$, these observations do not demand that $\text{Cp}^*_2\text{Zr}(\eta^2\text{-E}_2)(\text{CO})$ are intermediates in the direct reaction between $\text{Cp}^*_2\text{Zr}(\text{CO})_2$, E and $\text{C}_5\text{H}_5\text{N}$ to give $\text{Cp}^*_2\text{Zr}(\text{E})(\text{NC}_5\text{H}_5)$.

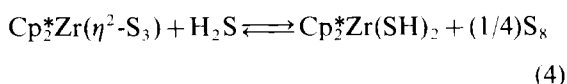


In addition to chalcogen abstraction, chalcogens may also be added to the $[\text{Zr}(\eta^2\text{-E}_2)]$ moiety. Thus, the complexes $\text{Cp}_2^*\text{Zr}(\eta^2\text{-E}_2)(\text{CO})$ ($\text{E} = \text{S}, \text{Se}, \text{Te}$) react with excess chalcogen to give the trichalcogenido derivatives $\text{Cp}_2^*\text{Zr}(\eta^2\text{-E}_3)$ (Scheme 2). Interestingly, for the tritellurido derivative, the reaction is reversible and addition of CO (1 atm) to $\text{Cp}_2^*\text{Zr}(\eta^2\text{-Te}_3)$ regenerates $\text{Cp}_2^*\text{Zr}(\eta^2\text{-Te}_2)(\text{CO})$ over a period of one day at room temperature (eq. (3)). However, the trisulfido and triselenido derivatives do not react with CO to give $\text{Cp}_2^*\text{Zr}(\eta^2\text{-E}_2)(\text{CO})$ under similar conditions.



Although $\text{Cp}_2^*\text{Zr}(\eta^2\text{-S}_3)$ and $\text{Cp}_2^*\text{Zr}(\eta^2\text{-Se}_3)$ do not react directly with CO to give $\text{Cp}_2^*\text{Zr}(\eta^2\text{-E}_2)(\text{CO})$, the dichalcogenido-carbonyl complexes may be formed by reaction with $\text{Cp}_2^*\text{Zr}(\text{CO})_2$ (Scheme 2). Overall, the role of $\text{Cp}_2^*\text{Zr}(\text{CO})_2$ in this reaction is to (i) provide a source of CO, and (ii) act as a trap for the liberated sulfur or selenium, thereby promoting the formation of $\text{Cp}_2^*\text{Zr}(\eta^2\text{-E}_2)(\text{CO})$. However, since $\text{Cp}_2^*\text{Zr}(\eta^2\text{-E}_2)(\text{CO})$ undergoes a secondary reaction with excess $\text{Cp}_2^*\text{Zr}(\text{CO})_2$,⁷¹ a mixture of products is eventually obtained. Nevertheless, the observed reaction between $\text{Cp}_2^*\text{Zr}(\eta^2\text{-E}_3)$ and $\text{Cp}_2^*\text{Zr}(\text{CO})_2$ is still significant because it demonstrates that it is possible to abstract a chalcogen from the four-membered rings of $\text{Cp}_2^*\text{Zr}(\eta^2\text{-S}_3)$ and $\text{Cp}_2^*\text{Zr}(\eta^2\text{-Se}_3)$.

Finally, the trisulfido $\text{Cp}_2^*\text{Zr}(\eta^2\text{-S}_3)$ reacts with excess H_2S in benzene at *ca.* 80°C to give the bis(hydrosulfido) complex $\text{Cp}_2^*\text{Zr}(\text{SH})_2$ (eq. (4)). However, the reaction does not proceed to completion and only generates an equilibrium mixture with $\text{Cp}_2^*\text{Zr}(\eta^2\text{-S}_3)$, an observation which is consistent with the report that $\text{Cp}_2^*\text{Zr}(\text{SH})_2$ also reacts with excess sulfur to give $\text{Cp}_2^*\text{Zr}(\eta^2\text{-S}_3)$.⁵⁷



Structure of the tetragonal modification of $\text{Cp}_2^*\text{Zr}(\eta^2\text{-Te}_2)(\text{CO})$

The asymmetric unit of the tetragonal modification of $\text{Cp}_2^*\text{Zr}(\eta^2\text{-Te}_2)(\text{CO})$ is composed of a half-molecule which resides on a crystallographic two-fold axis. However, since $\text{Cp}_2^*\text{Zr}(\eta^2\text{-Te}_2)(\text{CO})$ itself does not possess a molecular C_2 axis, the structure is necessarily disordered. The nature of the disorder is such that the $\text{Cp}_2^*\text{Zr}(\eta^2\text{-Te}_2)(\text{CO})$ molecules pack so that the carbonyl ligands are statistically distributed about the crystallographic two-fold axis, which bisects the two Zr—Te bond vectors. As such, the disorder could be satisfactorily modeled by refining the carbonyl ligand in a general position with half-occupancy. The ORTEP drawing shown in Fig. 10 illustrates that reasonable thermal parameters are obtained for this refinement procedure. However, the derived bond lengths are not consistent with the values obtained for the triclinic modification described above, as summarized in

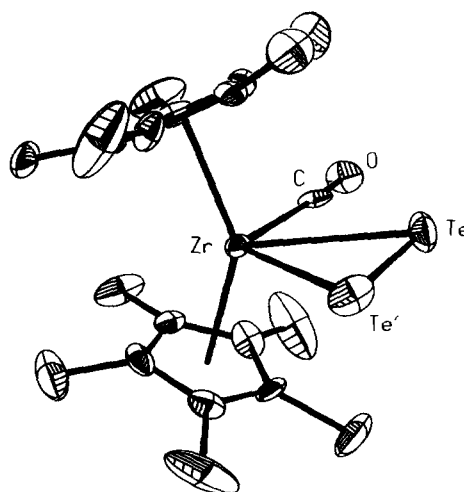


Fig. 10. ORTEP drawing of the tetragonal modification of $\text{Cp}_2^*\text{Zr}(\eta^2\text{-Te}_2)(\text{CO})$. Only one position of the disordered CO ligand (with half-occupancy) is shown.

Table 10. Specifically, the Zr—C bond length [2.47(2) Å] of the tetragonal modification is considerably longer than the average value in the triclinic modification [2.241(6) Å], even though the C—O bond lengths are similar, 1.13(3) and 1.123(9) Å, respectively.

It is important to understand the origin of the differences in the derived Zr—C bond lengths, especially since it is only fortuitous that an ordered triclinic modification existed. One possible origin of the different bond lengths is crystallographic disorder, since it is now well-established that disorder may result in the derivation of incorrect bond lengths.^{72,73} Of particular relevance to the present study, disorder between CN and X (X = Cl, Br) groups as a result of cocrystallizing [Tp^{Bu}]⁺ZnCN with small quantities of [Tp^{Bu}]⁺ZnCl or [Tp^{Bu}]⁺ZnBr is manifested by the observation that the derived Zn—C bond lengths for the cocrystallized system are longer than that in the pure compound, while the derived C—N bond lengths are shorter than that in the pure compound.⁷⁴ Thus, although it is plausible that the long Zr—C bond length observed for the tetragonal Cp₂⁺Zr(η²-Te₂)(CO) modification is a consequence of disorder with some impurity, such an explanation is not consistent with the fact that the C—O bond length is effectively unperturbed from the value in the ordered triclinic system.

A possible solution to the problem was suggested by examination of the thermal parameter of the zirconium in the plane defined by the [Zr(η²-Te₂)(CO)] moiety (Fig. 11). Thus, the thermal parameter of zirconium appears to be slightly (but by no means, excessively) elongated along the Zr—CO bond vector, which thereby suggests that the zirconium itself, in addition to the carbonyl ligand, may also be disordered about the two-fold axis. The disorder was subsequently modeled by allowing the Zr atom to refine in a general position off the two-fold axis, with a site occupancy factor of 0.5.⁷⁵ The result of this refinement procedure is illustrated in Fig. 12, which indicates that the Zr atom with half-occupancy refines with reasonable thermal parameters. Importantly, the consequence of allowing

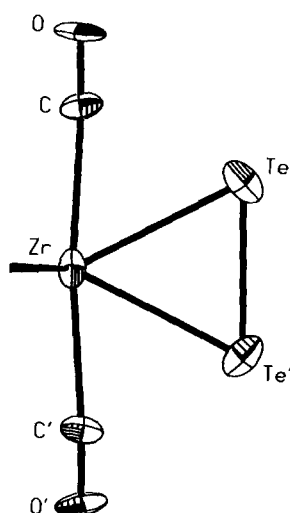


Fig. 11. ORTEP drawing in the [Zr(η²-Te₂)CO] plane of the tetragonal modification of Cp₂⁺Zr(η²-Te₂)(CO), with Zr refined on the two-fold axis. Cp* ligands are not shown for clarity. Each CO ligand has half-occupancy.

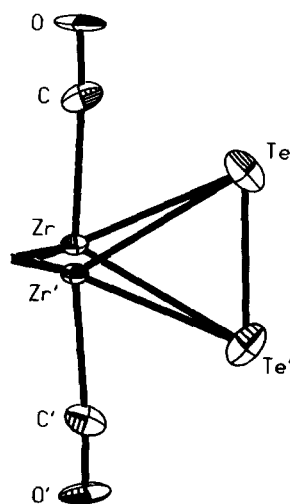


Fig. 12. ORTEP drawing in the [Zr(η²-Te₂)CO] plane of the tetragonal modification of Cp₂⁺Zr(η²-Te₂)(CO), with Zr refined off the two-fold axis. Cp* ligands are not shown for clarity. The Zr and CO moieties have half-occupancy.

Table 10. Average bond lengths (Å) for triclinic and tetragonal Cp₂⁺Zr(η²-Te₂)(CO)

	Zr—C	C—O	Zr—Te	Te—Te
Triclinic	2.241(7)	1.123(9)	2.96(1)	2.69(2)
Tetragonal, Zr on two-fold	2.47(2)	1.13(3)	2.942(2)	2.642(2)
Tetragonal, Zr off two-fold	2.24(2)	1.12(3)	2.95(9) ^a	2.640(2)

^a The individual Zr—Te bond lengths are 2.848(5) and 3.047(5) Å.

the Zr to refine in a general position is such that the Zr—C bond length is now reduced considerably from 2.47(2) to 2.24(2) Å, effectively identical to the average value for the ordered triclinic modification [2.241(6) Å]. It is also important that the C—O bond length [1.12(3) Å] is effectively unperturbed by this refinement procedure. A further consequence of allowing the Zr atom to refine off the two-fold axis is that the derived Zr—Te bond lengths are no longer equal, with values 2.848(5) and 3.047(5) Å. However, since it is likely that the ditellurido ligand is also disordered, the derived Zr—Te bond lengths are not particularly meaningful, and no attempt was made to resolve their disorder.

Disorder of the type exhibited by tetragonal $\text{Cp}_2^*\text{Zr}(\eta^2\text{-Te}_2)(\text{CO})$, whereby a central metal atom is unnecessarily constrained to refining on a symmetry element, is not uncommon, and some related examples include Ru(*meso*-tetraphenylporphyrin)(CO)(EtOH),⁷⁶ Fe(*meso*-tetraphenylporphyrin)(OH)(OH₂),⁷⁷ and W(PMe₃)₄(CH₃)(CCH₃).^{78,79} The importance of the present example is that $\text{Cp}_2^*\text{Zr}(\eta^2\text{-Te}_2)(\text{CO})$ represents a rare example of a structurally characterized non-classical transition metal carbonyl compound. The database on such complexes is extremely small, and it is conceivable that the long Zr—C bond length of 2.47(2) Å could have been accepted as being true, especially since a long bond length would have been anticipated due to the poor ability of the Zr^{IV} center to back-bond to the carbonyl ligand. The present study serves to emphasize further the deceptive nature of crystallographic disorder on derived bond lengths.

CONCLUSION

In summary, a series of non-classical zirconium carbonyl complexes $\text{Cp}_2^*\text{Zr}(\eta^2\text{-E}_2)(\text{CO})$ (E = S, Se, Te) has been prepared by the reactions of $\text{Cp}_2^*\text{Zr}(\text{CO})_2$ with the elemental chalcogens. The carbonyl complexes $\text{Cp}_2^*\text{Zr}(\eta^2\text{-E}_2)(\text{CO})$ are characterized by ν_{CO} stretching frequencies in the range 2057–2006 cm⁻¹, which are indicative of little $d \rightarrow \pi^*$ back-bonding compared to that for the d^2 derivative $\text{Cp}_2^*\text{Zr}(\text{CO})_2$ (1945 and 1852 cm⁻¹). On the basis that the ν_{CO} stretching frequencies decrease in the order S > Se > Te, and that the rate of CO exchange for $\text{Cp}_2^*\text{Zr}(\eta^2\text{-Te}_2)(\text{CO})$ is slower than for the sulfido and selenido analogues, the strength of the zirconium–carbonyl interaction is proposed to increase across the series S < Se < Te.

The dichalcogenido moiety [$\text{Zr}(\eta^2\text{-E}_2)$] in these complexes is reactive, and chalcogen transfer both to and from the [$\text{Zr}(\eta^2\text{-E}_2)$] group has been observed. Thus, the complexes $\text{Cp}_2^*\text{Zr}(\eta^2\text{-E}_2)(\text{CO})$ (E = S, Se, Te) react with (i) excess chalcogen to

give the trichalcogenido derivatives $\text{Cp}_2^*\text{Zr}(\eta^2\text{-E}_3)$, and (ii) $\text{Cp}_2^*\text{Zr}(\text{CO})_2$ in the presence of pyridine to give the terminal chalcogenido derivatives $\text{Cp}_2^*\text{Zr}(\text{E})(\text{NC}_5\text{H}_5)$.

The trichalcogenido complexes $\text{Cp}_2^*\text{Zr}(\eta^2\text{-E}_3)$ appear to represent the thermodynamically most stable species in the presence of excess chalcogen. Nevertheless, chalcogen abstraction from $\text{Cp}_2^*\text{Zr}(\eta^2\text{-E}_3)$ to give $\text{Cp}_2^*\text{Zr}(\eta^2\text{-E}_2)(\text{CO})$ may be achieved by reaction with (i) $\text{Cp}_2^*\text{Zr}(\text{CO})_2$ for all derivatives, and (ii), CO for the specific case of $\text{Cp}_2^*\text{Zr}(\eta^2\text{-Te}_3)$.

$\text{Cp}_2^*\text{Zr}(\eta^2\text{-Te}_2)(\text{CO})$ exists in two different crystalline modifications, namely triclinic and tetragonal. Interestingly, the derived Zr—CO bond lengths for the two structures were significantly different, while the C—O bond lengths for each were similar. Thus, an exceptionally long Zr—CO bond length of 2.47(2) Å was observed for the tetragonal form, compared to the value of 2.241(7) Å for the triclinic form. The derivation of a long Zr—CO bond length for the tetragonal structure was ascertained to be a consequence of crystallographic disorder, and appropriate modeling resulted in the determination of a reduced bond length of 2.24(2) Å, similar to that of 2.241(7) Å for the ordered triclinic modification. The structure of the tetragonal modification of $\text{Cp}_2^*\text{Zr}(\eta^2\text{-Te}_2)(\text{CO})$, therefore, provides an interesting example of crystallographic disorder which, in the absence of a suitable model, results in the derivation of a completely inaccurate metal–carbonyl bond length, yet still derives a perfectly reasonable C—O bond length.

EXPERIMENTAL SECTION

General considerations

All manipulations were performed using a combination of glovebox, high-vacuum or Schlenk techniques.⁸⁰ Solvents were purified and degassed by standard procedures. ¹H NMR spectra were measured on Varian VXR 200, 300 and 400 spectrometers. ¹³C (75.4 MHz), ⁷⁷Se (57.2 MHz), and ¹²⁵Te (94.6 MHz) NMR spectra were measured on a Varian VXR 300 spectrometer. Solutions of Ph₂Se₂ (δ 460.0 ppm) and Me₂Te (δ 0 ppm) in C₆D₆ were used as external references and the chemical shifts are reported relative to Me₂Se and Me₂Te. IR spectra were recorded on a Perkin–Elmer 1600 spectrophotometer and the data are reported in cm⁻¹. Mass spectra were obtained on a Nermag R10-10 mass spectrometer using chemical ionization (NH₃ or CH₄) techniques. Elemental analyses were measured using a Perkin–Elmer 2400 CHN

Elemental Analyzer. $\text{Cp}_2^*\text{Zr}(\text{CO})_2$ was prepared as reported previously.⁸¹ ^{13}C O (99%) was obtained from Cambridge Isotope Laboratories, Inc., Andover, MA.

Synthesis of $\text{Cp}_2^*\text{Zr}(\eta^2\text{-S}_2)(\text{CO})$

A mixture of $\text{Cp}_2^*\text{Zr}(\text{CO})_2$ (0.63 g, 1.51 mmol) and sulfur (0.08 g, 2.50 mmol) in toluene (*ca.* 5 cm³) was heated at 85°C for *ca.* 7 h. The mixture was allowed to cool to room temperature overnight, over which period small red–orange microcrystals were deposited. After cooling further to –78°C, the mixture was filtered and the crystals were washed with pentane (3 × 5 cm³) at room temperature and dried *in vacuo*. A further crop of $\text{Cp}_2^*\text{Zr}(\eta^2\text{-S}_2)(\text{CO})$ was also obtained from the combined filtrate and washings by cooling to –78°C. Total yield of $\text{Cp}_2^*\text{Zr}(\eta^2\text{-S}_2)(\text{CO})$: 0.29 g (51%, based on sulfur). Analysis found: C, 55.6; H, 6.8%; Calc. for $\text{Cp}_2^*\text{Zr}(\eta^2\text{-S}_2)(\text{CO})$: C, 55.6; H, 6.7%. IR data (KBr pellet): 2905 (vs), 2725 (w), 2057 (vs) (ν_{CO}), 1487 (m), 1432 (s), 1376 (vs), 1158 (w), 1064 (w), 1023 (s), 952 (w), 806 (w), 597 (w), 523 (w), 487 (w). ¹H NMR (C_6D_6): δ 1.70 [30H, s, 2 { $\eta^5\text{-C}_5(\text{CH}_3)_5$ }]. ¹³C NMR (C_6D_6): δ 11.5 [10C, q, ¹J_{C-H} = 127, 2{ $\eta^5\text{-C}_5(\text{CH}_3)_5$ }], 115.4 [10C, s, 2{ $\eta^5\text{-C}_5(\text{CH}_3)_5$ }], 218.5 [1C, s, Zr–CO].

Synthesis of $\text{Cp}_2^*\text{Zr}(\eta^2\text{-Se}_2)(\text{CO})$

A mixture of $\text{Cp}_2^*\text{Zr}(\text{CO})_2$ (0.30 g, 0.72 mmol) and selenium powder (0.110 g, 1.39 mmol) in toluene (*ca.* 5 cm³) was heated at 90°C for *ca.* 14 h. The mixture was allowed to cool slowly to –78°C, thereby depositing $\text{Cp}_2^*\text{Zr}(\eta^2\text{-Se}_2)(\text{CO})$ as orange crystals. The mixture was filtered and the crystals were washed with pentane (3 × 5 cm³) at room temperature and dried *in vacuo*. A further crop of $\text{Cp}_2^*\text{Zr}(\eta^2\text{-Se}_2)(\text{CO})$ was also obtained from the combined filtrate and washings by cooling to –78°C. Total yield of $\text{Cp}_2^*\text{Zr}(\eta^2\text{-Se}_2)(\text{CO})$: 0.21 g (54%, based on Se). Analysis found: C, 46.1; H, 5.7%; Calc. for $\text{Cp}_2^*\text{Zr}(\eta^2\text{-Se}_2)(\text{CO})$: C, 46.1; H, 5.5%. IR data (KBr pellet): 2896 (s), 2037 (vs) (ν_{CO}), 1431 (m), 1376 (s), 1022 (m), 730 (w), 596 (w). ¹H NMR (C_6D_6): δ 1.75 [30H, s, 2 { $\eta^5\text{-C}_5(\text{CH}_3)_5$ }]. ¹³C NMR (C_6D_6): δ 12.0 [10C, q, ¹J_{C-H} = 127, 2{ $\eta^5\text{-C}_5(\text{CH}_3)_5$ }], 114.9 [10C, s, 2{ $\eta^5\text{-C}_5(\text{CH}_3)_5$ }], 222.5 [1C, s, Zr–CO].

Synthesis of $\text{Cp}_2^*\text{Zr}(\eta^2\text{-Te}_2)(\text{CO})$

A mixture of $\text{Cp}_2^*\text{Zr}(\text{CO})_2$ (0.318 g, 0.76 mmol) and tellurium powder (0.118 g, 0.92 mmol) in toluene (*ca.* 5 cm³) was heated at 80°C for 1.5 days.

The mixture was allowed to cool slowly to –78°C, thereby depositing $\text{Cp}_2^*\text{Zr}(\eta^2\text{-Te}_2)(\text{CO})$ as dark red crystals. The mixture was filtered and the crystals were washed with pentane (3 × 5 cm³) at room temperature and dried *in vacuo*. A further crop of $\text{Cp}_2^*\text{Zr}(\eta^2\text{-Te}_2)(\text{CO})$ was also obtained from the combined filtrate and washings by cooling to –78°C. Total yield of $\text{Cp}_2^*\text{Zr}(\eta^2\text{-Te}_2)(\text{CO})$: 0.24 g (53%, based on Te). Analysis found: C, 39.4; H, 4.9%; Calc. for $\text{Cp}_2^*\text{Zr}(\eta^2\text{-Te}_2)(\text{CO})$: C, 39.1; H, 4.7%. IR data (KBr pellet): 2884 (vs), 2369 (w), 2006 (vs) (ν_{CO}), 1829 (w), 1482 (m), 1430 (s), 1373 (vs), 775 (w), 652 (w), 437 (w), 406 (w). ¹H NMR (C_6D_6): δ 1.81 [30H, s, 2 { $\eta^5\text{-C}_5(\text{CH}_3)_5$ }]. ¹³C NMR (C_6D_6): δ 13.2 [10C, q, ¹J_{C-H} = 128, 2{ $\eta^5\text{-C}_5(\text{CH}_3)_5$ }], 114.2 [10C, s, 2{ $\eta^5\text{-C}_5(\text{CH}_3)_5$ }], 231.8 [1C, s, Zr–CO].

Synthesis of $\text{Cp}_2^*\text{Zr}(\eta^2\text{-S}_3)$

A mixture of $\text{Cp}_2^*\text{Zr}(\text{CO})_2$ (0.21 g, 0.50 mmol) and sulfur powder (0.05 g, 1.56 mmol) in pentane (*ca.* 5 cm³) was stirred at room temperature overnight. The volatile components were removed *in vacuo*, giving $\text{Cp}_2^*\text{Zr}(\eta^2\text{-S}_3)$ as an orange solid. Yield of $\text{Cp}_2^*\text{Zr}(\eta^2\text{-S}_3)$: 0.21 g (90%). ¹H NMR (C_6D_6): δ 1.71 [30H, s, 2 { $\eta^5\text{-C}_5(\text{CH}_3)_5$ }]. $\text{Cp}_2^*\text{Zr}(\eta^2\text{-S}_3)$ has been previously synthesized by alternative procedures.^{56–58}

Synthesis of $\text{Cp}_2^*\text{Zr}(\eta^2\text{-Se}_3)$

A mixture of $\text{Cp}_2^*\text{Zr}(\text{CO})_2$ (0.21 g, 0.50 mmol) and selenium powder (0.17 g, 2.15 mmol) in pentane (*ca.* 10 cm³) was heated at 65°C (*CARE*) overnight in a glass ampoule sealed with a Teflon valve. The blood red mixture that was obtained was filtered, and the residue was extracted with toluene. The pentane and toluene extracts were combined and the volatile components were removed *in vacuo*, giving $\text{Cp}_2^*\text{Zr}(\eta^2\text{-Se}_3)$ as a red solid. Yield of $\text{Cp}_2^*\text{Zr}(\eta^2\text{-Se}_3)$: 0.27 g (90%). Analysis found: C, 40.0; H, 5.2%; Calc. for $\text{Cp}_2^*\text{Zr}(\eta^2\text{-Se}_3)$: C, 40.1; H, 5.1%. IR data (KBr pellet): 2968 (s), 2893 (vs), 2716 (w), 1485 (s), 1428 (vs), 1372 (vs), 1062 (w), 1019 (s), 597 (w), 407 (w). ¹H NMR (C_6D_6): δ 1.75 [30H, s, 2 { $\eta^5\text{-C}_5(\text{CH}_3)_5$ }]. ¹³C NMR (C_6D_6): δ 12.4 [10C, q, ¹J_{C-H} = 127, 2{ $\eta^5\text{-C}_5(\text{CH}_3)_5$ }], 118.5 [10C, s, 2{ $\eta^5\text{-C}_5(\text{CH}_3)_5$ }]. ⁷⁷Se NMR (C_6D_6): 136 [s, ¹J_{Se-Se} = 184, central Se], 555 [s, ¹J_{Se-Se} = 184, 2 lateral Se].

Synthesis of $\text{Cp}_2^*\text{Zr}(\eta^2\text{-Te}_3)$

A mixture of $\text{Cp}_2^*\text{Zr}(\text{CO})_2$ (0.25 g, 0.60 mmol) and tellurium powder (0.39 g, 3.06 mmol) in toluene

(ca. 10 cm³) was heated at 85°C for 3 days, removing the gaseous products periodically.⁸² The mixture was filtered and the volatile components were removed from the dark purple filtrate *in vacuo*, giving Cp₂*Zr(η²-Te₃) as a dark purple microcrystalline solid. Yield of Cp₂*Zr(η²-Te₃): 0.25 g (55%). Analysis found: C, 33.0; H, 4.4%; Calc. for Cp₂*Zr(η²-Te₃): C, 32.3; H, 4.1%. IR data (KBr pellet): 2896 (vs), 1441 (s), 1372 (vs), 1019 (s), 382 (w). ¹H NMR (C₆D₆): δ 1.89 [30H, s, 2{η⁵-C₅(CH₃)₅}]. ¹³C NMR (C₆D₆): δ 14.2 [10C, q, ¹J_{C-H} = 127, 2{η⁵-C₅(CH₃)₅}], 119.4 [10C, s, 2{η⁵-C₅(CH₃)₅}]. ¹²⁵Te NMR (C₆D₆): -401 [s, ¹J_{Te-Te} = 1800, central Te], 297 [s, ¹J_{Te-Te} = 1800, 2 lateral Te].

Cp₂*Zr(η²-E₂)(CO) and CO exchange studies

¹³C NMR spectroscopy was used to demonstrate CO exchange between Cp₂*Zr(η²-E₂)(¹³CO) and ¹²CO. Thus, solutions of Cp₂*Zr(η²-E₂)(¹³CO) (ca. 40 mg) in C₆D₆ (ca. 1 cm³) were exposed to ¹²CO (1 atm) and monitored by ¹³C NMR spectroscopy, which demonstrated a reduction in the intensity of the resonance attributable to the [Zr—¹³CO] moiety. Degenerate exchange studies between Cp₂*Zr(η²-E₂)(¹³CO) and ¹³CO were performed on samples prepared by exposing solutions of Cp₂*Zr(η²-E₂)(¹³CO) in C₆D₆ to an identical pressure of ¹³CO.

Chalcogen abstraction from Cp₂*Zr(η²-E₂)(CO): formation of Cp₂*Zr(E)(NC₅H₅)

A solution of Cp₂*Zr(η²-E₂)(CO) (E = S, Se, Te) (ca. 15 mg), Cp₂*Zr(CO)₂ (ca. 15 mg) and C₅H₅N (10 μl) in C₆D₆ (1 cm³) was heated at 80°C. The reaction was monitored by ¹H NMR spectroscopy, which demonstrated the formation of Cp₂*Zr(E)(NC₅H₅) after ca. 1 day.

Chalcogen addition to Cp₂*Zr(η²-E₂)(CO): formation of Cp₂*Zr(η²-E₃)

A solution of Cp₂*Zr(η²-E₂)(CO) (E = S, Se, Te) (ca. 25 mg) in C₆D₆ was treated with excess E (ca. 5–25 mg). The reaction was monitored by ¹H NMR spectroscopy, which demonstrated the complete formation of Cp₂*Zr(η²-E₃) after 4 h at 60°C for E = S, overnight at 60°C for E = Se, and 1 day at 125°C for E = Te.

Reaction between Cp₂*Zr(η²-Te₃) and CO: formation of Cp₂*Zr(η²-Te₂)(CO)

A solution of Cp₂*Zr(η²-Te₃) (ca. 10 mg) in C₆D₆ was treated with CO (1 atm). The reaction was

monitored by ¹H NMR spectroscopy which demonstrated the clean formation of Cp₂*Zr(η²-Te₂)(CO) over a period of 1 day at room temperature. The corresponding reactions of Cp₂*Zr(η²-S₃) and Cp₂*Zr(η²-Se₃) indicated no formation of Cp₂*Zr(η²-E₂)(CO) either at room temperature or 60°C for ca. 12 h.

Reaction between Cp₂*Zr(η²-E₃) and Cp₂*Zr(CO)₂: formation of Cp₂*Zr(η²-E₂)(CO)

A mixture of Cp₂*Zr(η²-E₃) (ca. 15 mg) and Cp₂*Zr(CO)₂ (ca. 10 mg) in C₆D₆ (1 cm³) was monitored using ¹H and ¹³C NMR spectroscopy, which demonstrated the formation of, *inter alia*, Cp₂*Zr(η²-E₂)(CO) (E = S, 1 day at room temperature; E = Se, 1 h at 55°C; E = Te, 2 h at room temperature).

Reaction between Cp₂*Zr(η²-S₃) and H₂S: formation of Cp₂*Zr(SH)₂

A solution of Cp₂*Zr(η²-S₃) (ca. 10 mg) in C₆D₆ (1 cm³) was treated with H₂S (1 atm). The mixture was heated at 80°C for 1.5 days, giving a mixture of Cp₂*Zr(η²-S₃) and Cp₂*Zr(SH)₂. No further change was observed upon further heating for several days.

X-ray structure determination of triclinic Cp₂*Zr(η²-Te₂)(CO)

Crystal data, data collection and refinement parameters for Cp₂*Zr(η²-Te₂)(CO) are summarized in Table 11. A single crystal of Cp₂*Zr(η²-Te₂)(CO) was mounted in a glass capillary and placed on a Nicolet R3m diffractometer. The unit cell was determined by the automatic indexing of 25 centered reflections and confirmed by examination of the axial photographs. Intensity data were collected using graphite monochromated Mo-K_α X-radiation (λ = 0.71073 Å). Check reflections were measured every 100 reflections, and the data were scaled accordingly and corrected for Lorentz, polarization, and absorption effects. The structure was solved by direct methods using SHELXTL PC™. Systematic absences were consistent with the space groups P1 (No. 1) and P $\bar{1}$ (No. 2), of which the choice P $\bar{1}$ (No. 2) was made, and confirmed by the success of the solution. Hydrogen atoms were included in calculated positions (*d*(C–H) = 0.96 Å; *U*_{iso}(H) = 0.08 Å²).

Table 11. Crystal and intensity collection data for $\text{Cp}_2^*\text{Zr}(\eta^2\text{-Te}_2)(\text{CO})$

$\text{Cp}_2^*\text{Zr}(\eta^2\text{-Te}_2)(\text{CO})$		
Formula	$\text{C}_{21}\text{H}_{30}\text{OTe}_2\text{Zr}$	$\text{C}_{21}\text{H}_{30}\text{OTe}_2\text{Zr}$
Formula weight	644.9	644.9
Lattice	Triclinic	Tetragonal
Cell constants		
a (Å)	9.507(2)	15.186(2)
b (Å)	16.052(3)	15.186(2)
c (Å)	17.268(3)	9.926(2)
α (°)	115.74(2)	90.0
β (°)	104.75(2)	90.0
γ (°)	93.68(2)	90.0
V (Å ³)	2249(1)	2289(1)
Z	4	4
Radiation, λ (Å)	Mo- K_α (0.71073)	Mo- K_α (0.71073)
Space group	$P\bar{1}$ (No. 2)	$P\bar{4}n2$ (No. 118)
ρ (calc.) (g cm ⁻³)	1.905	1.871
μ (Mo- K_α) (cm ⁻¹)	30.39	29.85
2θ range (°)	3–45	3–55
No. of data	6050 [$F > 4\sigma(F)$]	1173 [$F > 4\sigma(F)$]
No. of parameters	452	132 [125] ^a
Goodness-of-fit	1.32	1.36 [1.33] ^a
R	0.0383	0.0418 [0.0418] ^a
R_w	0.0512	0.0556 [0.0547] ^a

^a Numbers in square brackets are the values for refining Zr on the two-fold axis.

X-ray structure determination of tetragonal $\text{Cp}_2^*\text{Zr}(\eta^2\text{-Te}_2)(\text{CO})$

Crystal data, data collection and refinement parameters are summarized in Table 11, and the general procedure is as described for triclinic $\text{Cp}_2^*\text{Zr}(\eta^2\text{-Te}_2)(\text{CO})$. Systematic absences were consistent with the space groups $P4_2nm$ (No. 102), $P\bar{4}n2$ (No. 118), and $P4_2/mnm$ (No. 136). The latter space group was excluded on the basis of the molecular symmetry, and attempts to solve the structure in space group $P4_2nm$ (No. 102) were unsuccessful. A satisfactory solution was, however, obtained by using space group $P\bar{4}n2$ (No. 118). The structure was initially refined with the Zr on the two-fold axis, and subsequently refined off the two-fold axis. The occupancy of the Zr and CO ligand was fixed at 0.5 for both refinement procedures. Inversion of configuration indicated the correct absolute structure.

X-ray structure determination of $\text{Cp}_2^*\text{Zr}(\eta^2\text{-E}_3)$ (E = S, Se)

Crystal data, data collection and refinement parameters are summarized in Table 12, and the general procedure is as described for

Table 12. Crystal and intensity collection data for $\text{Cp}_2^*\text{Zr}(\eta^2\text{-E}_3)$

	$\text{Cp}_2^*\text{Zr}(\eta^2\text{-S}_3)$	$\text{Cp}_2^*\text{Zr}(\eta^2\text{-Se}_3)$	$\text{Cp}_2^*\text{Zr}(\eta^2\text{-Te}_3)$
Formula	$\text{C}_{20}\text{H}_{30}\text{S}_3\text{Zr}$	$\text{C}_{20}\text{H}_{30}\text{Se}_3\text{Zr}$	$\text{C}_{20}\text{H}_{30}\text{Te}_3\text{Zr}$
Formula weight	457.9	598.6	744.5
Lattice	Monoclinic	Monoclinic	Orthorhombic
Cell constants			
a (Å)	8.910(2)	9.134(3)	20.004(5)
b (Å)	14.017(3)	13.937(3)	15.666(2)
c (Å)	17.450(4)	17.610(3)	14.711(4)
α (°)	90.0	90.0	90.0
β (°)	104.03(2)	104.84(2)	90.0
γ (°)	90.0	90.0	90.0
V (Å ³)	2114(1)	2167(1)	4610(2)
Z	4	4	8
Radiation (λ , Å)	Mo- K_α (0.71073)	Mo- K_α (0.71073)	Mo- K_α (0.71073)
Space group	$P2_1/c$ (No. 14)	$P2_1/c$ (No. 14)	$Pna2_1$ (No. 33)
ρ (calc.) (g cm ⁻³)	1.44	1.83	2.145
μ (Mo- K_α) (cm ⁻¹)	8.0	59.1	41.99
2θ range (°)	3–50	3–50	4–45
No. of data	2832 [$F > 6\sigma(F)$]	2524 [$F > 6\sigma(F)$]	1746 [$F > 5\sigma(F)$]
No. of parameters	218	218	195
Goodness-of-fit	1.138	1.345	1.04
R	0.0319	0.0480	0.0477
R_w	0.0434	0.0576	0.0535

$\text{Cp}_2^*\text{Zr}(\eta^2\text{-Te}_2)(\text{CO})$, with the exception that the structure was solved using SHELXTL.⁸³ Systematic absences were consistent uniquely with the space group $P2_1/c$ (No. 14).

X-ray structure determination of $\text{Cp}_2^\text{Zr}(\eta^2\text{-Te}_3)$*

Crystal data, data collection and refinement parameters are summarized in Table 12, and the general procedure is as described for $\text{Cp}_2^*\text{Zr}(\eta^2\text{-Te}_2)(\text{CO})$. Systematic absences were consistent with the space groups $Pna2_1$ (No. 33) and $Pnam$ (No. 62). After no success using $Pnam$ (No. 62), the choice $Pna2_1$ (No. 33) was made and confirmed by the success of the solution. Furthermore, the two crystallographically independent but chemically similar molecules are not related by symmetry, thereby excluding the centrosymmetric space group alternative $Pnam$ (No. 62). Inversion of configuration indicated the correct choice of absolute structure.

Acknowledgments—We thank the U.S. Department of Energy, Office of Basic Energy Sciences (#DE-FG02-93ER14339), and the donors of the Petroleum Research Fund, administered by the American Chemical Society, for partial support of this research. We are grateful to Professors R. F. Jordan, J. M. Stryker, and D. H. Berry for copies of their manuscripts (refs 22, 24 and 26b, respectively) prior to publication, and we thank Dr J. C. Huffman for very helpful comments regarding the structure of $\text{Cp}_2^*\text{Zr}(\eta^2\text{-Te}_2)(\text{CO})$. G. P. is the recipient of an A. P. Sloan Research Fellowship (1991–1993), a Camille and Henry Dreyfus Teacher-Scholar Award (1991–1996), and a Presidential Faculty Fellowship Award (1992–1997).

REFERENCES

- J. P. Collman, L. S. Hegedus, J. R. Norton and R. G. Finke, *Principles and Applications of Organotransition Metal Chemistry*. University Science Books, Mill Valley, California (1987).
- C. Elschenbroich and A. Salzer, *Organometallics*, 2nd edn. VCH, New York (1992).
- D. M. P. Mingos, in *Comprehensive Organometallic Chemistry* (Edited by G. Wilkinson, F. G. A. Stone and E. W. Abel), Vol. 3, Section 19-2. Pergamon Press, Oxford (1982).
- The relative importance of the σ -donor and π -acceptor interactions has, however, been the subject of considerable debate. See ref. 3 and (a) D. E. Sherwood Jr and M. B. Hall, *Inorg. Chem.* 1983, **22**, 93–100; (b) B. E. Bursten, D. G. Freier and R. F. Fenske, *Inorg. Chem.* 1980, **19**, 1810–1811; (c) D. E. Sherwood Jr and M. B. Hall, *Inorg. Chem.* 1980, **19**, 1805–1809; (d) J. B. Johnson and W. G. Klemperer, *J. Am. Chem. Soc.* 1977, **99**, 7132–7137.
- G. W. Bethke and M. K. Wilson, *J. Chem. Phys.* 1957, **26**, 1118–1130.
- D. Tevault and K. Nakamoto, *Inorg. Chem.* 1976, **15**, 1282–1287.
- (a) W. Manchot and H. Gall, *Chem. Ber.* 1925, **58B**, 2175–2178; (b) P. G. Jones, *Z. Naturforsch.* 1982, **37B**, 823–824; (c) F. Calderazzo, *Pure Appl. Chem.* 1978, **50**, 49–53.
- C. Mealli, C. S. Arcus, J. L. Wilkinson, T. J. Marks and J. A. Ibers, *J. Am. Chem. Soc.* 1976, **98**, 711–718.
- For other examples of copper(I) carbonyl complexes, see: J. S. Thompson and J. F. Whitney, *Inorg. Chem.* 1984, **23**, 2813–2819, and references cited therein.
- For CO adsorbed on surfaces of ZnO, see: K. L. D'Amico, M. Trenary, N. D. Shinn, E. I. Solomon and F. R. McFeely, *J. Am. Chem. Soc.* 1982, **104**, 5102–5105.
- For a brief review, see: L. Weber, *Angew. Chem., Int. Ed. Engl.* 1994, **33**, 1077–1078.
- P. K. Hurlburt, O. P. Anderson and S. H. Strauss, *J. Am. Chem. Soc.* 1991, **113**, 6277–6278.
- (a) P. K. Hurlburt, J. J. Rack, S. F. Dec, O. P. Anderson and S. H. Strauss, *Inorg. Chem.* 1993, **32**, 373–374; (b) P. K. Hurlburt, J. J. Rack, J. S. Luck, S. F. Dec, J. D. Webb, O. P. Anderson and S. H. Strauss, *J. Am. Chem. Soc.* 1994, **116**, 10003–10014.
- H. Willner and F. Aubke, *Inorg. Chem.* 1990, **29**, 2195–2200.
- M. Adelhelm, W. Bacher, E. G. Höhn and E. Jacob, *Chem. Ber.* 1991, **124**, 1559–1561.
- H. Willner, J. Schaebs, G. Hwang, F. Mistry, R. Jones, J. Trotter and F. Aubke, *J. Am. Chem. Soc.* 1992, **114**, 8972–8980.
- H. Willner, M. Bodenbinder, C. Wang and F. Aubke, *J. Chem. Soc., Chem. Commun.* 1994, 1189–1190.
- Some d^0 and d^1 carbonyl complexes of titanium include $[\{\text{Cp}_2\text{Ti}(\text{CO})\}_2\{\mu\text{-(NC)}_2\text{C}=\text{C}(\text{CN})_2\}]$ $[(\text{NC})_2\text{C}=\text{C}(\text{CN})_2]$,^{18a} $\text{Cp}_2\text{Ti}(\text{CO})\text{Cl}$,^{18b} $\text{Cp}_2\text{Ti}(\text{C}_6\text{F}_5)(\text{CO})$,^{18c} and $\text{Cp}_2^*\text{Ti}(\text{CO})\text{Cl}$.^{18c} The complex $\text{Cp}_2\text{Ti}(\text{CO})(\text{PhCCPh})$ may also be considered to be a d^0 metallocyclopropene derivative.^{18d} (a) B. Demersman, M. Pankowski, G. Bouquet and M. Bigorgne, *J. Organomet. Chem.* 1976, **117**, C10–C12; (b) E. U. Van Raaij, C. D. Schmulbach and H. H. Brintzinger, *J. Organomet. Chem.* 1987, **328**, 275–285; (c) E. J. M. De Boer, L. C. Ten Cate, A. G. J. Staring and J. H. Teuben, *J. Organomet. Chem.* 1979, **181**, 61–68; (d) G. Fachinetti, C. Floriani, F. Marchetti and M. Mellini, *J. Chem. Soc., Dalton Trans.* 1978, 1398–1403.
- Non-classical carbonyl complexes are also known for some of the later transition metals, in which the d -electrons may not be available for back-bonding. See: (a) F. Calderazzo and D. Belli Dell'Amico, *Pure Appl. Chem.* 1986, **58**, 561–566; (b) F. Calderazzo, *J. Organomet. Chem.* 1990, **400**, 303–320; (c) J. D. Scott and R. J. Puddephatt, *Organometallics* 1986, **5**, 1253–1257; (d) R. Usón, J. For-

- niés, M. Tomás and B. Menjón, *Organometallics* 1985, **4**, 1912–1914; (e) B. P. Andreini, D. Belli Dell'Amico, F. Calderazzo, M. G. Venturi, G. Pelizzi and A. Segre, *J. Organomet. Chem.* 1988, **354**, 357–368; (f) G. Hwang, C. Wang, F. Aubke, H. Willner and M. Bodenbinder, *Can. J. Chem.* 1993, **71**, 1532–1536.
20. (a) J. M. Manriquez, D. R. McAlister, R. D. Sanner and J. E. Bercaw, *J. Am. Chem. Soc.* 1976, **98**, 6733–6735; (b) J. M. Manriquez, D. R. McAlister, R. D. Sanner and J. E. Bercaw, *J. Am. Chem. Soc.* 1978, **100**, 2716–2724.
21. For the hafnium analogue, $\text{Cp}_2^*\text{HfH}_2(\text{CO})$, see: D. M. Roddick, M. D. Fryzuk, P. F. Seidler, G. L. Hillhouse and J. E. Bercaw, *Organometallics* 1985, **4**, 97–104.
22. Z. Guo, D. C. Swenson, A. S. Guram and R. F. Jordan, *Organometallics* 1994, **13**, 766–773.
23. Jordan also obtained spectroscopic evidence for the non-classical cation $[\text{Cp}_2\text{Zr}\{\eta^2\text{-CH}(\text{Me})(6\text{-ethylpyrid-2-yl})\text{-C,N}\}(\text{CO})]^+$ in 1992, but this complex could not be isolated. See: A. S. Guram, D. C. Swenson and R. F. Jordan, *J. Am. Chem. Soc.* 1992, **114**, 8991–8996.
24. D. M. Antonelli, E. B. Tjaden and J. M. Stryker, *Organometallics* 1994, **13**, 763–765.
25. The complex $\text{Cp}_2\text{Zr}(\eta^2\text{-Me}_2\text{SiNBu}^t)(\text{CO})$ has also been reported (ref. 26). However, a value of 1797 cm^{-1} for ν_{CO} is indicative of extensive back-bonding into the $\text{CO } \pi^*$ orbital in this complex (see text).
26. (a) L. J. Procopio, P. J. Carroll and D. H. Berry, *J. Am. Chem. Soc.* 1991, **113**, 1870–1872; (b) L. J. Procopio, P. J. Carroll and D. H. Berry, *Polyhedron* 1995, **14**, 45–55.
27. (a) W. A. Howard, M. Waters and G. Parkin, *J. Am. Chem. Soc.* 1993, **115**, 4917–4918; (b) W. A. Howard and G. Parkin, *J. Am. Chem. Soc.* 1994, **116**, 606–615.
28. W. A. Howard and G. Parkin, *J. Organomet. Chem.* 1994, **472**, C1–C4.
29. Abbreviations: $\text{Cp}^\dagger = \text{Cp}^*$ or $\text{Cp}^{\text{Et}*}$; $\text{Cp}^* = \eta^5\text{-C}_5\text{Me}_5$; $\text{Cp}^{\text{Et}*} = \eta^5\text{-C}_5\text{Me}_4\text{Et}$.
30. The hafnium oxo derivatives $\text{Cp}_2^*\text{Hf}(\text{O})(\text{NC}_5\text{H}_5)$ are prepared by the reactions of the tellurido complexes $\text{Cp}_2^*\text{Hf}(\text{Te})(\text{NC}_5\text{H}_5)$ with N_2O . See ref. 28.
31. (a) M. J. Carney, P. J. Walsh and R. G. Bergman, *J. Am. Chem. Soc.* 1990, **112**, 6426–6428; (b) M. J. Carney, P. J. Walsh, F. J. Hollander and R. G. Bergman, *Organometallics* 1992, **11**, 761–777.
32. M. R. Smith III, P. T. Matsunaga and R. A. Andersen, *J. Am. Chem. Soc.* 1993, **115**, 7049–7050.
33. Our present studies do not distinguish the sequence of formation of $\text{Cp}_2^*\text{Zr}(\eta^2\text{-E}_2)(\text{CO})$ and $\text{Cp}_2^*\text{Zr}(\eta^2\text{-E}_3)$, since these complexes are interconvertible under the reaction conditions.
34. Typical $\text{Cp}_2^*\text{Zr}(\text{CO})_2$:E stoichiometries are in the range ca. 1:1.4 to 1:1.9.
35. It should also be noted that $\text{Cp}_2^*\text{Zr}(\text{CO})_2$ has previously been reported to be unreactive towards N_2O . See: F. Bottomley, D. F. Drummond, G. O. Egharevba and P. S. White, *Organometallics* 1986, **5**, 1620–1625.
36. It is, however, possible that one of the products of the reaction may be a metallated complex that is analogous to $[\text{Cp}^*\text{Ti}](\mu\text{-}\eta^5, \eta^1\text{-C}_5\text{Me}_4\text{CH}_2)(\mu\text{-O})_2$, which is the product of the reaction between Cp_2^*Ti and N_2O . See: F. Bottomley, G. O. Egharevba, I. J. B. Lin and P. S. White, *Organometallics* 1985, **4**, 550–553.
37. For example, see refs 20, 21 and also: (a) G. Erker, *Acc. Chem. Res.* 1984, **17**, 103–109; (b) J. Schwartz and J. A. Labinger, *Angew. Chem., Int. Ed. Engl.* 1976, **15**, 333–340; (c) P. Hofmann, P. Stauffert, M. Frede and K. Tasumi, *Chem. Ber.* 1989, **122**, 1559–1577.
38. (a) R. L. DeKock, A. C. Sarapu and R. F. Fenske, *Inorg. Chem.* 1971, **10**, 38–43; (b) M. B. Hall and R. F. Fenske, *Inorg. Chem.* 1972, **11**, 1619–1624.
39. The ν_{CO} stretching frequencies of the complexes $\text{Re}_2\text{Br}_2(\text{CO})_6(\text{E}_2\text{Ph}_2)$ also decrease in the order $\text{S} > \text{Se} > \text{Te}$. See ref. 7c.
40. J. A. Marsella, C. J. Curtis, J. E. Bercaw and K. G. Caulton, *J. Am. Chem. Soc.* 1980, **102**, 7244–7246.
41. D. J. Sikora, M. D. Rausch, R. D. Rogers and J. L. Atwood, *J. Am. Chem. Soc.* 1981, **103**, 1265–1267.
42. $r_{\text{cov}}(\text{sp } \text{C}) = 0.60 \text{ \AA}$; $r_{\text{cov}}(\text{sp}^3 \text{C}) = 0.77 \text{ \AA}$; $r_{\text{cov}}(\text{Si}) = 1.17 \text{ \AA}$; $r_{\text{cov}}(\text{S}) = 1.04 \text{ \AA}$; $r_{\text{cov}}(\text{Se}) = 1.17 \text{ \AA}$; $r_{\text{cov}}(\text{Te}) = 1.37 \text{ \AA}$. A value of 1.51 \AA has been suggested for the single bond covalent radius of Zr in the zirconocene system (see ref. 27b). The van der Waals radii of atoms are effectively 0.8 \AA greater than their covalent radii. L. Pauling, *The Nature of The Chemical Bond*, 3rd edn. Cornell University Press, Ithaca, New York (1960).
43. It is, however, well known that neutral main group and late transition metal carbonyl derivatives may exhibit ν_{CO} stretching frequencies higher than that in free CO, e.g. $\text{Au}(\text{CO})\text{Cl}$ (2162 cm^{-1} in CH_2Cl_2) and $\text{Pt}(\text{CO})_2\text{Cl}_2$ (2180 cm^{-1} in CH_2Cl_2). For example, see ref. 7c.
44. A value of 183.4 ppm has been cited. See: G. E. Maciel, J. L. Dallas and D. P. Miller, *J. Am. Chem. Soc.* 1976, **98**, 5074–5082.
45. Related correlations have also been observed between ^{13}C NMR shift and C—O force constants for other systems. See, for example: (a) B. E. Mann, *J. Chem. Soc., Dalton Trans.* 1973, 2012–2015; (b) O. A. Gansow, B. Y. Kimura, G. R. Dobson and R. A. Brown, *J. Am. Chem. Soc.* 1971, **93**, 5922–5924; (c) O. A. Gansow, D. A. Schexnayder and B. Y. Kimura, *J. Am. Chem. Soc.* 1972, **94**, 3406–3408; (d) M. H. Chisholm, H. C. Clark, L. E. Manzer, J. B. Stothers and J. E. H. Ward, *J. Am. Chem. Soc.* 1973, **95**, 8574–8583; (e) G. M. Bodner and L. J. Todd, *Inorg. Chem.* 1974, **13**, 1335–1338.
46. For a general comment concerning the rationalization of chemical shifts of carbon atoms bound to transition metals, see: J. Evans and J. R. Norton, *Inorg. Chem.* 1974, **13**, 3042–3043.
47. (a) J. L. Templeton and B. C. Ward, *J. Am. Chem. Soc.* 1980, **102**, 3288–3290; (b) J. L. Templeton, *Adv. Organomet. Chem.* 1989, **29**, 1–100.
48. For example, (tetra-*p*-tolylporphyrin)Ti($\eta^2\text{-S}_2$),^{48a,b}

- and $[\text{Ph}_4\text{P}][\text{CpTi}(\eta^2\text{-S}_2)(\eta^2\text{-S}_5)]$.^{48c} (a) R. Guillard, C. Ratti, A. Tabard, P. Richard, D. Dubois and K. M. Kadish, *Inorg. Chem.* 1990, **29**, 2532–2540; (b) C. Ratti, P. Richard, A. Tabard and R. Guillard, *J. Chem. Soc., Chem. Commun.* 1989, 69–70; (c) A. Müller, E. Krickemeyer, A. Sprafke, N. H. Schladerbeck and H. Bögge, *Chimia* 1988, **42**, 68–69.
49. (a) R. Guillard, J.-M. Latour, C. Lecomte, J.-C. Marchon, J. Protas and D. Ripoll, *Inorg. Chem.* 1978, **17**, 1228–1237; (b) D. Schwarzenbach, *Inorg. Chem.* 1970, **9**, 2391–2397; (c) H. Mimoun, M. Postel, F. Casabianca, J. Fischer and A. Mitschler, *Inorg. Chem.* 1982, **21**, 1303–1306; (d) D. Schwarzenbach, *Helv. Chim. Acta* 1972, **55**, 2990–3004; (e) M. Postel, F. Casabianca, Y. Gauffreteau and J. Fischer, *Inorg. Chim. Acta* 1986, **113**, 173–180; (f) H. Manohar and D. Schwarzenbach, *Helv. Chim. Acta* 1974, **57**, 1086–1095; (g) D. Schwarzenbach and K. Girgis, *Helv. Chim. Acta* 1975, **58**, 2391–2398; (h) P. Jeske, G. Haselhorst, T. Weyhermüller, K. Wieghardt and B. Nuber, *Inorg. Chem.* 1994, **33**, 2462–2471.
50. In addition to mononuclear $[\text{M}(\eta^2\text{-Te}_2)]$ coordination, the ditellurido ligand is known to coordinate in a variety of other coordination modes. See for example: (a) L. C. Roof and J. W. Kolis, *Chem. Rev.* 1993, **93**, 1037–1080; (b) M. A. Ansari, J. C. Bollinger and J. A. Ibers, *J. Am. Chem. Soc.* 1993, **115**, 3838–3839; (c) B. Schreiner, K. Dehnicke and D. Fenske, *Z. Anorg. Allg. Chem.* 1993, **619**, 1127–1131; (d) R. E. Bachman and K. H. Whitmire, *Organometallics* 1993, **12**, 1988–1992; (e) O. Scheidsteger, G. Huttner, K. Dehnicke and J. Pebler, *Angew. Chem., Int. Ed. Engl.* 1985, **24**, 428; (f) M. G. Kanatzidis and S.-P. Huang, *Coord. Chem. Rev.* 1994, **130**, 509–621.
51. G. Llabres, O. Dideberg and L. Dupont, *Acta Cryst.* 1972, **B28**, 2438–2444.
52. M. R. Spirlet, G. Van Den Bossche, O. Dideberg and L. Dupont, *Acta Cryst.* 1979, **B35**, 1727–1729.
53. For further comparison, the Te—Te bond lengths in the $[\text{M}(\eta^2\text{-Te}_2)]$ complexes are intermediate between those of Te_2 in the gas phase $[2.59(2) \text{ \AA}]$ ^{53a} and elemental Te, in the solid state $[2.835(2) \text{ \AA}]$.^{53b} Furthermore, the Te—Te bond lengths in binary tellurides are typically ca. 2.81 \AA .^{53c} (a) L. R. Maxwell and V. M. Mosley, *Phys. Rev.* 1940, **57**, 21–23; (b) P. Cherin and P. Unger, *Acta Crystallogr.* 1967, **23**, 670–671; (c) P. Böttcher, *Angew. Chem., Int. Ed. Engl.* 1988, **27**, 759–772.
54. For a lucid discussion on the use of the term resonance structure as applied to the latter situation, see ref. 6 in B. R. Bender, J. R. Norton, M. M. Miller, O. P. Anderson and A. K. Rappé, *Organometallics* 1992, **11**, 3427–3434.
55. D. M. Roddick and J. E. Bercaw, *Chem. Ber.* 1989, **122**, 1579–1587.
56. A. Shaver and J. M. McCall, *Organometallics* 1984, **3**, 1823–1829.
57. R. Broussier, M. Rigoulet, R. Amardeil, G. Delmas and B. Gautheron, *Phosphorus, Sulfur, and Silicon* 1993, **82**, 55–60.
58. $\text{Cp}^*_2\text{Zr}(\eta^2\text{-S}_3)$ has also been cited in another publication, but few details were given. See: R. Beckhaus and K.-H. Thiele, *Z. Anorg. Allg. Chem.* 1989, **573**, 195–198.
59. W. A. Howard and G. Parkin, *Organometallics* 1993, **12**, 2363–2366.
60. A. Shaver, J. M. McCall, P. H. Bird and U. Siriwardane, *Acta Cryst.* 1991, **C47**, 659–661.
61. P. H. Bird, J. M. McCall, A. Shaver and U. Siriwardane, *Angew. Chem., Int. Ed. Engl.* 1982, **21**, 384–385.
62. N. Albrecht and E. Weiss, *J. Organomet. Chem.* 1988, **355**, 89–98.
63. A. Shaver, J. M. McCall, V. W. Day and S. Vollmer, *Can. J. Chem.* 1987, **65**, 1676–1680.
64. The structures of the titanium complexes $(\eta^5\text{-C}_5\text{H}_4\text{SiMe}_3)_2\text{Ti}(\eta^2\text{-S}_5)$,^{64a} $\text{Cp}_2\text{Ti}(\eta^2\text{-S}_5)$,^{64b,c} and $\text{Cp}_2\text{Ti}(\eta^2\text{-Se}_5)$,^{64d} have also been determined by X-ray diffraction. (a) N. Klouras, S. Voliotis and G. Germain, *Acta Cryst.* 1984, **C40**, 1791–1793; (b) F. G. Muller, J. L. Petersen and L. F. Dahl, *J. Organomet. Chem.* 1976, **111**, 91–112; (c) E. F. Epstein, I. Bernal and H. Köpf, *J. Organomet. Chem.* 1971, **26**, 229–245; (d) D. Fenske, J. Adel and K. Dehnicke, *Z. Naturforsch.* 1987, **42b**, 931–933.
65. M. Björgvinsson and G. J. Schrobilgen, *Inorg. Chem.* 1991, **30**, 2540–2547.
66. The resonance at 555 ppm is also more intense than that at 136 ppm, but the observed ratio was slightly less than 2 : 1, presumably due to different relaxation times.
67. P. Pekonen, Y. Hiltunen and R. S. Laitinen, *Acta Chem. Scand.* 1989, **43**, 914–916.
68. For ⁷⁷Se NMR studies on $\text{Cp}_2\text{TiSe}_x\text{S}_{5-x}$, see: P. Pekonen, Y. Hiltunen, R. S. Laitinen and J. Valkonen, *Inorg. Chem.* 1991, **30**, 1874–1878.
69. The ¹³CO NMR signal is broadened to the extent that it cannot be observed under these conditions.
70. Other evidence which indicates that the complexes $\text{Cp}^*_2\text{Zr}(\eta^2\text{-E}_2)(\text{CO})$ dissociate CO readily is provided by the observation that solutions of the complexes decompose when the solvent is removed under vacuum.
71. $\text{Cp}^*_2\text{Zr}(\eta^2\text{-E}_2)(\text{CO})$ and $\text{Cp}^*_2\text{Zr}(\text{CO})_2$ also react in the absence of pyridine. The nature of the products, however, is not at present known with certainty.
72. G. Parkin, *Chem. Rev.* 1993, **93**, 887–911.
73. For a recent interesting example of compositional disorder in the peroxo compound $(\text{Me}_3\text{tacn})\text{Ti}(\eta^2\text{-O}_2)(\text{NCO})_2$ resulting in an anomalously short O—O bond length, see ref. 49h.
74. K. Yoon and G. Parkin, *Inorg. Chem.* 1992, **31**, 1656–1662.
75. The distance between the disordered Zr half-atoms is $0.449(11) \text{ \AA}$.
76. (a) J. J. Bonnet, S. S. Eaton, G. R. Eaton, R. H. Holm and J. A. Ibers, *J. Am. Chem. Soc.* 1973, **95**, 2141–2149; (b) D. Cullen, E. Meyer Jr, T. S. Srivastava and M. Tsutsui, *J. Chem. Soc., Chem. Commun.* 1972, 584–585.

77. (a) E. B. Fleischer, C. K. Miller and L. E. Webb, *J. Am. Chem. Soc.* 1964, **86**, 2342–2347; (b) J. L. Hoard, G. H. Cohen and M. D. Glick, *J. Am. Chem. Soc.* 1967, **89**, 1992–1996; (c) J. L. Hoard, M. J. Hamor, T. A. Hamor and W. S. Caughey, *J. Am. Chem. Soc.* 1965, **87**, 2312–2319.
78. (a) R. A. Jones, G. Wilkinson, A. M. R. Galas and M. B. Hursthouse, *J. Chem. Soc., Chem. Commun.* 1979, 926–927; (b) K. W. Chiu, R. A. Jones, G. Wilkinson, A. M. R. Galas, M. B. Hursthouse and K. M. A. Malik, *J. Chem. Soc., Dalton Trans.* 1981, 1204–1211.
79. For some related examples, see: (a) M. D. Glick, G. H. Cohen and J. L. Hoard, *J. Am. Chem. Soc.* 1967, **89**, 1996–1998; (b) A. Lachgar, D. S. Dudis and J. D. Corbett, *Inorg. Chem.* 1990, **29**, 2242–2246.
80. (a) J. P. McNally, V. S. Leong, and N. J. Cooper, in *Experimental Organometallic Chemistry* (Edited by A. L. Wayda and M. Y. Darensbourg), Chapter 2, pp. 6–23. American Chemical Society, Washington, DC (1987); (b) B. J. Burger and J. E. Bercaw, in *Experimental Organometallic Chemistry* (Edited by A. L. Wayda and M. Y. Darensbourg), Chapter 4, pp. 79–98. American Chemical Society, Washington, DC (1987).
81. D. J. Sikora, K. J. Moriarty and M. D. Rausch, *Inorg. Synth.* 1990, **28**, 248–257.
82. The reaction mixture was monitored by ^1H NMR spectroscopy in order to determine when the reaction was complete.
83. G. M. Sheldrick, SHELXTL, An Integrated System for Solving, Refining and Displaying Crystal Structures from Diffraction Data. University of Göttingen, Göttingen (1981).
84. (a) T. E. Waldman, L. Stahl, D. R. Wilson, A. M. Arif, J. P. Hutchinson and R. D. Ernst, *Organometallics* 1993, **12**, 1543–1552. (b) R. D. Ernst, personal communication.
85. M. D. Rausch, K. J. Moriarty, J. L. Atwood, W. E. Hunter and E. Samuel, *J. Organomet. Chem.* 1987, **327**, 39–54.
86. G. Fachinetti, G. Fochi and C. Floriani, *J. Chem. Soc., Chem. Commun.* 1976, 230–231.
87. J. T. Thomas and K. T. Brown, *J. Organomet. Chem.* 1976, **111**, 297–301.
88. A. Antiñolo, M. F. Lappert and D. J. W. Winterborn, *J. Organomet. Chem.* 1984, **272**, C37–C39.
89. Y. Wielstra, S. Gambarotta, J. B. Roedelof and M. Y. Chiang, *Organometallics* 1988, **7**, 2177–2182.
90. D. W. Blackburn, K. M. Chi, S. R. Frerichs, M. L. Tinkham and J. E. Ellis, *Angew. Chem., Int. Ed. Engl.* 1988, **27**, 437–438.
91. P. T. Barger, B. D. Santarsiero, J. Armantrout and J. E. Bercaw, *J. Am. Chem. Soc.* 1984, **106**, 5178–5186.
92. J. E. Ellis, K.-M. Chi, A.-J. DiMaio, S. R. Frerichs, J. R. Stenzel, A. L. Rheingold and B. S. Haggerty, *Angew. Chem., Int. Ed. Engl.* 1991, **30**, 194–196.
93. B. Demerseman, G. Bouquet and M. Bigorgne, *J. Organomet. Chem.* 1977, **132**, 223–229.
94. G. Erker, U. Dorf, C. Kruger and K. Angermund, *J. Organomet. Chem.* 1986, **301**, 299–312.
95. D. J. Sikora and M. D. Rausch, *J. Organomet. Chem.* 1984, **276**, 21–37.
96. K. I. Gell and J. Schwartz, *J. Am. Chem. Soc.* 1981, **103**, 2687–2695.
97. C. P. Casey, R. E. Palermo, R. F. Jordan and A. L. Rheingold, *J. Am. Chem. Soc.* 1985, **107**, 4597–4599. The low value of the ν_{CO} stretching frequency may be due to a semi-bridging interaction with Ru.
98. B. A. Kelsey and J. E. Ellis, *J. Am. Chem. Soc.* 1986, **108**, 1344–1345.
99. B. A. Kelsey and J. E. Ellis, *J. Chem. Soc., Chem. Commun.* 1986, 331–332.
100. J. E. Ellis and K.-M. Chi, *J. Am. Chem. Soc.* 1990, **112**, 6022–6025.
101. J. L. Atwood, R. D. Rogers, W. E. Hunter, C. Floriani, G. Fachinetti and A. Chiesi-Villa, *Inorg. Chem.* 1980, **19**, 3812–3817.
102. D. Rabinovich and G. Parkin, *J. Am. Chem. Soc.* 1993, **115**, 9822–9823.
103. J. H. Shin and G. Parkin, *Organometallics* 1994, **13**, 2147–2149.
104. M. Di Vaira, M. Peruzzini and P. Stoppioni, *Angew. Chem., Int. Ed. Engl.* 1987, **26**, 916–917.
105. G. Erker, T. Mühlenbernd, R. Nolte, J. L. Petersen, G. Tainturier and B. Gautheron, *J. Organomet. Chem.* 1986, **314**, C21–C24.
106. G. Erker, R. Nolte, G. Tainturier and A. Rheingold, *Organometallics* 1989, **8**, 454–460.